The Hanbury Brown–Twiss effect in electromagnetic beams

VRIJE UNIVERSITEIT

The Hanbury Brown–Twiss effect in electromagnetic beams

ACADEMISCH PROEFSCHRIFT

ter verkrijging van de graad Doctor aan
de Vrije Universiteit Amsterdam,
op gezag van de rector magnificus
prof.dr. V. Subramaniam,
in het openbaar te verdedigen
ten overstaan van de promotiecommissie
van de Faculteit der Bètawetenschappen
op maandag 14 oktober 2019 om 15.45 uur
in de aula van de universiteit,
De Boelelaan 1105

door

Gaofeng Wu

geboren te Chongqing, China

promotor: prof.dr. T.D. Visser

Samenstelling leescommissie:

Prof.dr. W.M.G. Ubachs,	Vrije Universiteit, Amsterdam, The Netherlands
Prof.dr. B.J. Hoenders,	Universiteit Groningen, The Netherlands
Prof.dr. A.T. Friberg,	University of Eastern Finland, Joensuu, Finland
Prof.dr. M.A. Alonso,	University of Rochester, Rochester, NY, USA
Dr. H.F. Schouten,	Vrije Universiteit, Amsterdam, The Netherlands

This work was financially supported by the China Scholarship Council.

Contents

Chapter 1

Introduction

1.1 The Hanbury Brown-Twiss effect

The exploration of space is a great dream of mankind. The observation of distant stars cannot be separated from the development of science and technology. Because the angular diameters that stars subtend at the surface of the Earth are exceedingly small, they cannot be measured directly even with the largest available telescopes. A. A. Michelson showed theoretically in 1890 and then, together with F. G. Pease [Michelson and Pease, 1921], demonstrated experimentally in the 1920s that the angular diameter of a star and, in principle, also the intensity across the stellar disk may be obtained with the help of an interferometer as shown schematically in Fig. (1.1). The principle of the technique may be understood as follows. Light from the star is incident on the outer mirrors M_1 and M_2 of the interferometer, is then reflected at two inner mirrors M_3 and M_4 and is brought to the back focal plane F of a telescope to interfere. The inner mirrors M_3 and M_4 are fixed while the outer mirrors M_1 and M_2 can be separated symmetrically in the direction joining M_3 and M_4.

The visibility of the interference fringes in the back focal plane F depends on the separation d between the mirrors M_1 and M_2. Michelson showed that if the stellar disk is rotationally symmetric and uniform, the visibility curve will have zeros for a certain separation distance d_0 [Wolf,

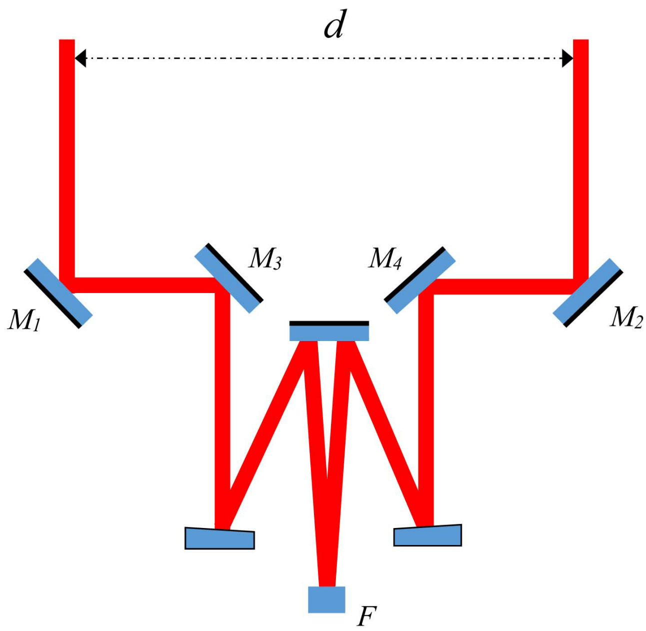

Figure 1.1: A schematic diagram of the Michelson stellar interferometer. The mirrors are denoted by the symbol M. F is the back focal plane of a telescope on which an interference pattern is formed.

2007]

$$d_0 = \frac{0.61\lambda_0}{\alpha}, \tag{1.1}$$

where λ_0 denotes a spectral wavelength component and α is the angular radius of the star. Thus, from a measurement of d_0 the angular diameter of the star may be determined. Since the time when the first Michelson stellar interferometer was built, this technique has been used mainly in radio astronomy. Although the principle has been applied with great success to map the radio sky, practical difficulties were encountered. The extremely small angles subtended by stars at the Earth's surface require the use of interferometers with baselines of several kilometers. Obviously, the required stability cannot be maintained over such long distances.

In the early 1950s a British engineer, Robert Hanbury Brown, considered the possibility of using a different type of stellar radio interferometer as shown in Fig. (1.2). Instead of interfering fields, he suggested to use *"intensity interfering"*. In the Hanbury Brown and Twiss interferometer the intensity arriving at antenna one and antenna two (or at two photoelectric detectors) are compared with each other by use of a correlator (multiplier). The first interferometer of this type was described in 1952 [Hanbury Brown *et al.*, 1952]. It was used to determine the angular diameters of two stars, using antennas separated by a few kilometers [Hanbury Brown and Twiss, 1954]. In 1956, Hanbury Brown and Twiss performed laboratory experiments to determine whether the technique worked also with visible light [Hanbury Brown and Twiss, 1956]. The experimental results agreed well with the theoretical predications for the intensity interfering of partially coherent light [Hanbury Brown and Twiss, 1958]. Ever since Hanbury Brown and Twiss (HBT) reported their results, the eponymous "HBT effect", has been applied in many branches of physics. The original description of the HBT effect, which assumes a scalar wave field and is described in [Wolf, 2007], was later generalized to electromagnetic beams, see [Mandel and Wolf, 1995] and [Shirai and Wolf, 2007; Volkov *et al.*, 2008; Al-Qasimi *et al.*, 2010; Hassinen *et al.*, 2011]. In this thesis we study the HBT effect in partially coherent electromagnetic beams. We therefore begin by briefly reviewing some concepts that will be used later on. In doing so we heavily borrow from [Mandel and Wolf, 1995; Wolf, 2007].

1.2 Vector coherence theory

In this section we will discuss the extension of scalar theory by taking the vector nature into account, i.e., we will combine the coherence and polarization of optical fields.

Let us consider a random electromagnetic beam propagating along the z-axis, from the plane $z = 0$ into the half space $z > 0$. The statistical properties of such a stochastic electromagnetic beam, in the space-frequency domain, is characterized by the *cross-spectral density matrix* which is de-

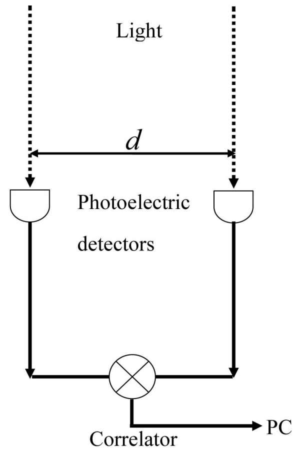

Figure 1.2: A diagram of an intensity interferometer.

fined as [Wolf, 2007]

$$\mathbf{W}(\mathbf{r}_1,\mathbf{r}_2,\omega) = \begin{pmatrix} W_{xx}(\mathbf{r}_1,\mathbf{r}_2,\omega) & W_{xy}(\mathbf{r}_1,\mathbf{r}_2,\omega) \\ W_{yx}(\mathbf{r}_1,\mathbf{r}_2,\omega) & W_{yy}(\mathbf{r}_1,\mathbf{r}_2,\omega) \end{pmatrix}, \tag{1.2}$$

with

$$W_{ij}(\mathbf{r}_1,\mathbf{r}_2,\omega) = \langle E_i^*(\mathbf{r}_1,\omega)E_j(\mathbf{r}_2,\omega)\rangle\,, \quad (i,j=x,y), \tag{1.3}$$

where $E_i(\mathbf{r},\omega)$ denotes a Cartesian component of the electric field at a point $\mathbf{r}$ at frequency ω, of a typical realization of the statistical ensemble representing the beam. The *spectral density* at one point $\mathbf{r}$ equals the sum of the expectation values of the squared modulus of both components, i.e.,

$$S(\mathbf{r},\omega) = \mathrm{Tr}\,\mathbf{W}(\mathbf{r},\mathbf{r},\omega), \tag{1.4}$$

where Tr denotes the trace. We regard the state of coherence of an electromagnetic beam as its ability to produce fringes in Young's experiment. Let us assume a stochastic, statistically stationary, electromagnetic beam which propagates close to the z-axis and is incident on an opaque screen A, containing two identical small openings at points $Q(\boldsymbol{\rho}_1)$ and $Q(\boldsymbol{\rho}_2)$ (see Fig. (1.3)). Let $\{\mathbf{E}(\mathbf{r},\omega)\}$ represent the statistical ensemble of the electric

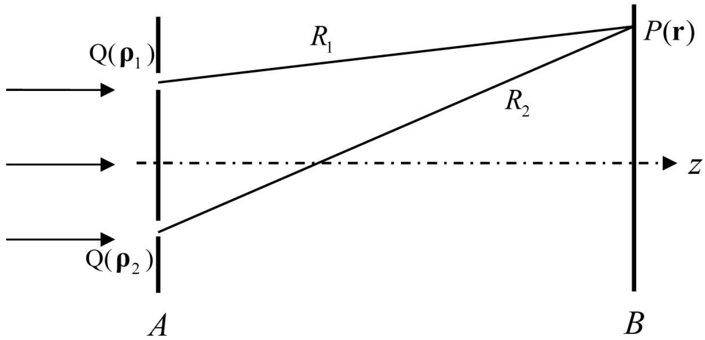

Figure 1.3: Notation relating to Young's interference experiment with stochastic electromagnetic beams.

vector at the point $P(\mathbf{r})$. A typical realization $\mathbf{E}(\mathbf{r},\omega)$ of this ensemble is given as

$$\mathbf{E}(\mathbf{r},\omega) = K_1\mathbf{E}(\boldsymbol{\rho}_1,\omega)e^{\mathrm{i}kR_1} + K_2\mathbf{E}(\boldsymbol{\rho}_2,\omega)e^{\mathrm{i}kR_2}, \tag{1.5}$$

where $\mathbf{E}(\boldsymbol{\rho}_\alpha,\omega)$, with $\alpha = 1, 2$, denotes the electric vector at point $Q(\boldsymbol{\rho}_\alpha)$, R_1 and R_2 are the distances from the points $Q(\boldsymbol{\rho}_1)$ and $Q(\boldsymbol{\rho}_2)$, respectively to the point $P(\mathbf{r})$. The propagation factors K_1 and K_2 are given as

$$K_\alpha \approx -\frac{\mathrm{i}}{\lambda R_\alpha} dA. \tag{1.6}$$

Here dA is the area of the two pinholes. On substituting Eqs. (1.2) and (1.5) into Eq. (1.4), we find that

$$\begin{aligned} S(\mathbf{r},\omega) &= S^{(1)}(\mathbf{r},\omega) + S^{(2)}(\mathbf{r},\omega) \\ &+ 2\sqrt{S^{(1)}(\mathbf{r},\omega)}\sqrt{S^{(2)}(\mathbf{r},\omega)}\mathrm{Re}[\eta(\rho_1,\rho_2,\omega)e^{\mathrm{i}k(R_2-R_1)}], \end{aligned} \tag{1.7}$$

where Re denotes the real part. Here $S^{(1)}(\mathbf{r},\omega)$ is the spectral density at the point $P(\mathbf{r})$ if only the pinhole at position $Q(\boldsymbol{\rho}_1)$ is open. Thus we have

$$S^{(1)}(\mathbf{r},\omega) = |K_1|^2 S(\boldsymbol{\rho}_1,\omega). \tag{1.8}$$

A strictly similar expression is obtained for the spectral density $S^{(2)}(\mathbf{r},\omega)$. We can see from Eq. (1.7), that the spectrum at the point $P(\mathbf{r})$ at the observation plane B contains three parts. The first two parts are the spectra of the two individual fields from points $Q(\boldsymbol{\rho}_1)$ and $Q(\boldsymbol{\rho}_2)$, respectively. The third part is the interference term with

$$\eta(\rho_1,\rho_2,\omega)=\frac{\mathrm{Tr}\,\mathbf{W}(\rho_1,\rho_2,\omega)}{\sqrt{S(\rho_1,\omega)}\sqrt{S(\rho_2,\omega)}}. \tag{1.9}$$

Here the term $\eta(\boldsymbol{\rho}_1,\boldsymbol{\rho}_2,\omega)$ is the *complex spectral degree of coherence* of the stochastic electromagnetic field between $Q(\boldsymbol{\rho}_1)$ and $Q(\boldsymbol{\rho}_2)$.

It should be noted that the spectral degree of coherence, $\eta(\boldsymbol{\rho}_1,\boldsymbol{\rho}_2,\omega)$ depends only on the diagonal elements of the cross-spectra density matrix $\mathbf{W}$. It is defined as the capability of the field at those points to produce interference fringes. According to the Fresnel-Argo laws, two orthogonally linearly polarized waves do not interfere. However, the fact that the two orthogonal components of a random electric field do not interfere with each other does not imply that these components are uncorrelated.

Although the off-diagonal elements of the cross-spectral density matrix $\mathbf{W}$ do not contribute to the degree of coherence, they play an import role in determining the polarization of beams. The polarization of a stochastic electromagnetic beam can be characterized by the *degree of polarization* that is defined as

$$P(\mathbf{r},\omega)=\sqrt{1-\frac{4\mathrm{Det}\,\mathbf{W}(\mathbf{r},\mathbf{r},\omega)}{[\mathrm{Tr}\,\mathbf{W}(\mathbf{r},\mathbf{r},\omega)]^2}}, \tag{1.10}$$

where Det denotes the determinant. The physical meaning of $P(\mathbf{r})$ is the ratio of the intensity of the completely polarized part to the total intensity. When $P(\mathbf{r})=0$ it means that the light is unpolarized, e.g. natural light, and when $P(\mathbf{r})=1$ it means that the light is completely polarized, e.g. linear polarization or circular polarization. When the value of $P(\mathbf{r})$ is between 0 and 1 the light is *partially polarized.* The state of polarization is further characterized by the Stokes parameters. For a stochastic electromagnetic beam, the *spectral Stokes parameters* are defined as

$$\langle S_0(\mathbf{r},\omega)\rangle = W_{xx}(\mathbf{r},\mathbf{r},\omega) + W_{yy}(\mathbf{r},\mathbf{r},\omega), \tag{1.11}$$
$$\langle S_1(\mathbf{r},\omega)\rangle = W_{xx}(\mathbf{r},\mathbf{r},\omega) - W_{yy}(\mathbf{r},\mathbf{r},\omega), \tag{1.12}$$
$$\langle S_2(\mathbf{r},\omega)\rangle = W_{xy}(\mathbf{r},\mathbf{r},\omega) + W_{yx}(\mathbf{r},\mathbf{r},\omega), \tag{1.13}$$
$$\langle S_3(\mathbf{r},\omega)\rangle = \mathrm{i}[W_{yx}(\mathbf{r},\mathbf{r},\omega) - W_{xy}(\mathbf{r},\mathbf{r},\omega)]. \tag{1.14}$$

These parameters can be determined experimentally in a similar way to how one determines the usual Stokes parameters, provided that the light is filtered to become quasi-monochromatic around the frequency ω.

1.3 Higher-order coherence

Let us begin by recalling the definition in the space-time domain of the second-order correlation function of a fluctuating scalar wavefield, represented by an analytic signal $V(\mathbf{r},t)$, namely

$$\Gamma(\mathbf{r}_1,\mathbf{r}_2,t_1,t_2) = \langle V^*(\mathbf{r}_1,t_1)V(\mathbf{r}_2,t_2)\rangle, \tag{1.15}$$

where the angular brackets now denote the time average. More explicitly,

$$\Gamma(\mathbf{r}_1,\mathbf{r}_2,t_1,t_2) = \iint V_1^* V_2\, p_2(V_1,V_2;\mathbf{r}_1,t_1;\mathbf{r}_2,t_2)\,\mathrm{d}^2V_1\mathrm{d}^2V_2, \tag{1.16}$$

where p_2 is the joint probability density of the fluctuating field at the two space-time points $(\mathbf{r}_1,t_1)$ and $(\mathbf{r}_2,t_2)$. Although this function is very useful for analyzing various coherence phenomena it cannot, in general, provide any information about the effects that involve probability densities of the third and higher orders. Among the most important quantities that are needed to elucidate coherence phenomena, which depend on the probability densities of order higher than the second, are the correlation functions

$$\begin{aligned}\Gamma^{(M,N)}&(\mathbf{r}_1,\mathbf{r}_2,...,\mathbf{r}_{M+N};t_1,t_2,...,t_{M+N})\\ &= \langle V^*(\mathbf{r}_1,t_1)V^*(\mathbf{r}_2,t_2)...V^*(\mathbf{r}_M,t_M)\\ &\times V(\mathbf{r}_{M+1},t_{M+1})V(\mathbf{r}_{M+2},t_{M+2})...V(\mathbf{r}_{M+N},t_{M+N})\rangle\end{aligned} \tag{1.17}$$

or, more explicitly,

$$\Gamma^{(M,N)}(\mathbf{r}_1, \mathbf{r}_2, ..., \mathbf{r}_{M+N}; t_1, t_2, ..., t_{M+N})$$
$$= \int ... \int_{(M+N)} V_1^* V_2^* ... V_M^* V_{M+1} V_{M+2} ... V_{M+N}$$
$$\times\, p_{M+N}(V_1, V_2, ..., V_{M+N}; \mathbf{r}_1, t_1; \mathbf{r}_2, t_2; ...; \mathbf{r}_{M+N}, t_{M+N})\, \mathrm{d}^2V_1 \mathrm{d}^2V_2 ... \mathrm{d}^2V_{M+V}. \tag{1.18}$$

We refer to $\Gamma^{(M,N)}$ as the *cross-correlation function (in the space-time domain)* of order (M, N) of the random field $V(\mathbf{r}, t)$.

To simplify the notation, we set

$$\begin{array}{rcll} \mathbf{r}_m, t_m & = & \mathbf{p}_m, & m = 1, 2, ..., M \\ \mathbf{r}_{M+n}, t_{M+n} & = & \mathbf{q}_n, & n = 1, 2, ..., N \end{array} \tag{1.19}$$

Eq. (1.17) may then be re-written as

$$\Gamma^{(M,N)}(\mathbf{p}_1, \mathbf{p}_2, ..., \mathbf{p}_M; \mathbf{q}_1, \mathbf{q}_2, ..., \mathbf{q}_N)$$
$$= \langle V^*(\mathbf{p}_1) V^*(\mathbf{p}_2) ... V^*(\mathbf{p}_M) V(\mathbf{q}_1) V(\mathbf{q}_2) ... V(\mathbf{q}_N) \rangle. \tag{1.20}$$

Based on the above definition, there are two important properties that can be derived, namely

$$\left[\Gamma^{(M,N)}(\mathbf{p}_1, \mathbf{p}_2, ..., \mathbf{p}_M; \mathbf{q}_1, \mathbf{q}_2, ..., \mathbf{q}_N)\right]^*$$
$$= \Gamma^{(N,M)}(\mathbf{q}_1, \mathbf{q}_2, ..., \mathbf{q}_N; \mathbf{p}_1, \mathbf{p}_2, ..., \mathbf{p}_M), \tag{1.21}$$

and

$$\left|\Gamma^{(M,N)}(\mathbf{p}_1, \mathbf{p}_2, ..., \mathbf{p}_M; \mathbf{q}_1, \mathbf{q}_2, ..., \mathbf{q}_N)\right|^2$$
$$\leq \Gamma^{(M,M)}(\mathbf{p}_1, \mathbf{p}_2, ..., \mathbf{p}_M; \mathbf{p}_1, \mathbf{p}_2, ..., \mathbf{p}_M)$$
$$\times\, \Gamma^{(N,N)}(\mathbf{q}_1, \mathbf{q}_2, ..., \mathbf{q}_N; \mathbf{q}_1, \mathbf{q}_2, ..., \mathbf{q}_N). \tag{1.22}$$

The above correlation functions are defined in the space-time domain. In a similar manner we can introduce space-frequency correlation functions [Mandel and Wolf, 1995] as

$$\Phi^{(M,N)}(\mathbf{r}_1, \mathbf{r}_2, ..., \mathbf{r}_{M+N}; \omega_1, \omega_2, ..., \omega_{M+N})$$
$$= \langle \tilde{V}^*(\mathbf{r}_1, \omega_1) \tilde{V}^*(\mathbf{r}_2, \omega_2) ... \tilde{V}^*(\mathbf{r}_M, \omega_M)$$
$$\times\, \tilde{V}(\mathbf{r}_{M+1}, \omega_{M+1}) \tilde{V}(\mathbf{r}_{M+2}, \omega_{M+2}) ... \tilde{V}(\mathbf{r}_{M+N}, \omega_{M+N}) \rangle, \tag{1.23}$$

where $\tilde{V}(\mathbf{r},\omega)$ is the Fourier transform of a fluctuating scalar field represented by an analytic signal $V(\mathbf{r},t)$ which is not necessarily stationary and let us represent it as

$$\tilde{V}(\mathbf{r},\omega) = \int_{-\infty}^{\infty} V(\mathbf{r},t)e^{\mathrm{i}\omega \mathrm{t}}\mathrm{d}t. \tag{1.24}$$

Hence we can obtain expression for the spectral cross-correlation functions in the form of the space-time correlation functions

$$\begin{aligned}
&\Phi^{(M,N)}(\mathbf{r}_1,\mathbf{r}_2,...,\mathbf{r}_{M+N};\omega_1,\omega_2,...,\omega_{M+N})\\
&= \int_{-\infty}^{\infty}\mathrm{d}t_1\int_{-\infty}^{\infty}\mathrm{d}t_2...\int_{-\infty}^{\infty}\mathrm{d}t_{M+N}\Gamma^{(M,N)}(\mathbf{r}_1,\mathbf{r}_2,...,\mathbf{r}_{M+N};t_1,t_2,...,t_{M+N})\\
&\times\prod_{j=1}^{M}\exp(-\mathrm{i}\omega_j t_j)\prod_{k=M+1}^{M+N}\exp(\mathrm{i}\omega_k t_k).
\end{aligned} \tag{1.25}$$

The space-time correlation functions $\Gamma^{(M,N)}$ will be invariant with respect to translation of the origin of time if we suppose that the field is stationary. We set

$$\tau_l = t_l - t_1, \quad (l = 2,3,...,M+N), \tag{1.26}$$

$\Gamma^{(M,N)}$ will be independent of t_1 and there is

$$\Gamma^{(M,N)} = \Gamma^{(M,N)}(\mathbf{r}_1,\mathbf{r}_2,...,\mathbf{r}_{M+N};\tau_2,\tau_3,...,\tau_{M+N}). \tag{1.27}$$

On substituting from Eq. (1.27) into Eq. (1.25) and carrying out the integration with respect to t_1, we get

$$\begin{aligned}
&\Phi^{(M,N)}(\mathbf{r}_1,\mathbf{r}_2,...,\mathbf{r}_{M+N};\omega_1,\omega_2,...,\omega_{M+N})\\
&= \delta(\omega_1+\omega_2+...+\omega_M-\omega_{M+1}-\omega_{M+2}-...\omega_{M+N})\\
&\times\int_{-\infty}^{\infty}\mathrm{d}\tau_2\int_{-\infty}^{\infty}\mathrm{d}\tau_3...\int_{-\infty}^{\infty}\mathrm{d}\tau_{M+N}\Gamma^{(M,N)}(\mathbf{r}_1,\mathbf{r}_2,...,\mathbf{r}_{M+N};\tau_2,\tau_3,...,\tau_{M+N})\\
&\times\prod_{j=2}^{M}\exp(-\mathrm{i}\omega_j\tau_j)\prod_{k=M+1}^{M+N}\exp(\mathrm{i}\omega_k\tau_k).
\end{aligned} \tag{1.28}$$

From Eq. (1.28), we find that

$$\Phi^{(M,N)}(\mathbf{r}_1, \mathbf{r}_2, ..., \mathbf{r}_{M+N}; \omega_1, \omega_2, ..., \omega_{M+N}) = 0, \tag{1.29}$$

unless

$$\omega_1 + \omega_2 + ... + \omega_M - \omega_{M+1} - \omega_{M+2} - ... - \omega_{M+N} = 0. \tag{1.30}$$

When the $M+N$ frequencies satisfy Eq. (1.30), the components $\tilde{V}(\mathbf{r}_j, \omega_j)$ will in general be correlated.

Let us return to the higher order correlation in the space-time domain. The cross correlation function $\Gamma^{(M,N)}$ can be expressed in terms of the lowest-order ones by use of the moment theorem if the fields obey Gaussian statistics and at each point is of zero mean. From the *Gaussian moment theorem* for a Gaussian random process, we get

$$\Gamma^{(M,N)}(\mathbf{p}_1, \mathbf{p}_2, ..., \mathbf{p}_M; \mathbf{q}_1, \mathbf{q}_2, ..., \mathbf{q}_N) = 0 \quad \text{if } N \neq M \tag{1.31}$$

and

$$\begin{aligned}&\Gamma^{(M,M)}(\mathbf{p}_1, \mathbf{p}_2, ..., \mathbf{p}_M; \mathbf{q}_1, \mathbf{q}_2, ..., \mathbf{q}_M)\\ &= \sum_\pi \Gamma^{(1,1)}(\mathbf{p}_{i_1}, \mathbf{q}_{j_1})\Gamma^{(1,1)}(\mathbf{p}_{i_2}, \mathbf{q}_{j_2})...\Gamma^{(1,1)}(\mathbf{p}_{i_M}, \mathbf{q}_{j_M}),\end{aligned} \tag{1.32}$$

where the subscripts i_p and j_q $(1 \leq i_p \leq M, 1 \leq j_q \leq M)$ are integers and $\sum_\pi$ denotes summation over all the $M!$ possible permutations of the subscripts. By substituting Eq. (1.32) into Eq. (1.25), we can express the spectral cross-correlation functions $\phi^{(M,N)}$ in terms of $\phi^{(1,1)}$ as

$$\phi^{(M,N)}(\mathbf{r}_1, \mathbf{r}_2, ..., \mathbf{r}_M; \mathbf{r}'_1, \mathbf{r}'_2, ..., \mathbf{r}'_N; \omega_1, \omega_2, ..., \omega_{M+N}) = 0 \quad \text{if } N \neq M \tag{1.33}$$

and

$$\begin{aligned}&\phi^{(M,M)}(\mathbf{r}_1, \mathbf{r}_2, ..., \mathbf{r}_M; \mathbf{r}'_1, \mathbf{r}'_2, ..., \mathbf{r}'_M; \omega_1, \omega_2, ..., \omega_{2M})\\ &= \sum_\pi \phi^{(1,1)}(\mathbf{r}_{i_1}, \mathbf{r}'_{j_1}; \omega_{i_1}, \omega_{j_1})\phi^{(1,1)}(\mathbf{r}_{i_2}, \mathbf{r}'_{j_2}; \omega_{i_2}, \omega_{j_2})\\ &\times ...\phi^{(1,1)}(\mathbf{r}_{i_M}, \mathbf{r}'_{j_M}; \omega_{i_M}, \omega_{j_M}).\end{aligned} \tag{1.34}$$

When we construct an ensemble of a monochromatic wave function $\{V(\mathbf{r},t) = U(\mathbf{r},\omega)e^{-\mathrm{i}\omega t}\}$, all of the same frequency ω, such that the *cross-spectral density function of order (M,M)* is equal to their cross-correlation function, i.e.,

$$\begin{aligned}
&\Phi^{(M,M)}(\mathbf{r}_1, \mathbf{r}_2, ..., \mathbf{r}_{2M}; \omega, \omega, ..., \omega)\\
&= W^{(M,M)}(\mathbf{r}_1, \mathbf{r}_2, ..., \mathbf{r}_{2M}; \omega, \omega, ..., \omega)\\
&= \langle U^*(\mathbf{r}_1, \omega)U^*(\mathbf{r}_2, \omega)...U^*(\mathbf{r}_M, \omega)\\
&\times U(\mathbf{r}_{M+1}, \omega)U(\mathbf{r}_{M+2}, \omega)...U(\mathbf{r}_{2M}, \omega)\rangle,
\end{aligned} \tag{1.35}$$

then, the cross-spectral density $W^{(M,M)}$ can be expressed in terms of the lowest-order ones by use of the moment theorem as

$$\begin{aligned}
&W^{(M,M)}(\mathbf{r}_1, \mathbf{r}_2, ..., \mathbf{r}_M; \mathbf{r}'_1, \mathbf{r}'_2, ..., \mathbf{r}'_M; \omega)\\
&= \sum_\pi W^{(1,1)}(\mathbf{r}_{i_1}, \mathbf{r}'_{j_1}; \omega)W^{(1,1)}(\mathbf{r}_{i_2}, \mathbf{r}'_{j_2}; \omega)...W^{(1,1)}(\mathbf{r}_{i_M}, \mathbf{r}'_{j_M}; \omega).
\end{aligned} \tag{1.36}$$

As an example, let us consider the case when $M = 2$. For this case, Eq. (1.36) gives

$$\begin{aligned}
W^{(2,2)}&(\mathbf{r}_1, \mathbf{r}_2; \mathbf{r}_1, \mathbf{r}_2; \omega)\\
&= W^{(1,1)}(\mathbf{r}_1, \mathbf{r}_1, \omega)W^{(1,1)}(\mathbf{r}_2, \mathbf{r}_2, \omega)\\
&+ W^{(1,1)}(\mathbf{r}_1, \mathbf{r}_2, \omega)W^{(1,1)}(\mathbf{r}_2, \mathbf{r}_1, \omega).
\end{aligned} \tag{1.37}$$

Since $W^{1,1}(\mathbf{r}_j, \mathbf{r}_j, \omega) = \langle I(\mathbf{r}_j)\rangle$ is the average value of the spectral density, Eq. (1.37) gives

$$W^{(2,2)}(\mathbf{r}_1, \mathbf{r}_2; \mathbf{r}_1, \mathbf{r}_2; \omega) = \langle I(\mathbf{r}_1)\rangle\langle I(\mathbf{r}_2)\rangle + |W^{(1,1)}(\mathbf{r}_1, \mathbf{r}_2, \omega)|^2 \tag{1.38}$$

Eq. (1.38) can be re-written as

$$W^{(2,2)}(\mathbf{r}_1, \mathbf{r}_2; \mathbf{r}_1, \mathbf{r}_2; \omega) = \langle I(\mathbf{r}_1)\rangle\langle I(\mathbf{r}_2)\rangle(1 + |\mu(\mathbf{r}_1, \mathbf{r}_2, \omega)|^2) \tag{1.39}$$

where

$$\mu(\mathbf{r}_1, \mathbf{r}_2, \omega) = \frac{W^{(1,1)}(\mathbf{r}_1, \mathbf{r}_2, \omega)}{\langle I(\mathbf{r}_1)\rangle\langle I(\mathbf{r}_2)\rangle} \tag{1.40}$$

is the *complex spectral degree of coherence* for scalar fields.

Let us introduce the intensity fluctuations

$$\Delta I(\mathbf{r},\omega) = I(\mathbf{r},\omega) - \langle I(\mathbf{r},\omega)\rangle. \tag{1.41}$$

Then the correlation of the intensity fluctuations is

$$\langle \Delta I(\mathbf{r}_1,\omega)\Delta I(\mathbf{r}_2,\omega)\rangle = \langle I(\mathbf{r}_1,\omega) I(\mathbf{r}_2,\omega)\rangle - \langle I(\mathbf{r}_1,\omega)\rangle\langle I(\mathbf{r}_2,\omega)\rangle \tag{1.42}$$

Recalling Eq. (1.37), one can obtain

$$\langle \Delta I(\mathbf{r}_1,\omega)\Delta I(\mathbf{r}_2,\omega)\rangle = |W^{(1,1)}(\mathbf{r}_1,\mathbf{r}_2,\omega)|^2. \tag{1.43}$$

From Eq. (1.43), it is seen that the correlation of the intensity fluctuations can be expressed as the second-order correlation $W^{(1,1)}(\mathbf{r}_1,\mathbf{r}_2,\omega)$. The normalized version of the correlation of the intensity fluctuations is

$$\frac{\langle \Delta I(\mathbf{r}_1,\omega)\Delta I(\mathbf{r}_2,\omega)\rangle}{\langle I(\mathbf{r}_1)\rangle\langle I(\mathbf{r}_2)\rangle} = |\mu(\mathbf{r}_1,\mathbf{r}_2,\omega)|^2. \tag{1.44}$$

Eq. (1.44) is the basic formula for intensity interferometry for thermal radiation. It shows that the absolute value of the spectral degree of coherence of the field at one pair of points may be determined from the measurements of the correlation of intensity fluctuations and the average spectral density at each point.

Up to now we have considered a scalar field $U(\mathbf{r},\omega)$ in this section, so that the preceding formulas cannot be used in the electromagnetic case. For the electromagnetic field, let $E_x(\mathbf{r},z,\omega)$ and $E_y(\mathbf{r},z,\omega)$ be the Cartesian components of the electric field at frequency ω along two mutually orthogonal x and y directions, perpendicular to the beam axis. The fluctuations of the intensity is now defined as

$$\begin{aligned}\Delta I(\mathbf{r},\omega) &= I(\mathbf{r},\omega) - \langle I(\mathbf{r},\omega)\rangle \\ &= |E_x(\mathbf{r},\omega)|^2 + |E_x(\mathbf{r},\omega)|^2 - \langle |E_x(\mathbf{r},\omega)|^2 + |E_x(\mathbf{r},\omega)|^2\rangle. \end{aligned} \tag{1.45}$$

For a stochastic electromagnetic field, assuming the field obeys Gaussian statistics, the correlation of intensity fluctuations at a pair of points is [Mandel and Wolf, 1995]

$$\langle \Delta I(\mathbf{r}_1,\omega)\Delta I(\mathbf{r}_2,\omega)\rangle = \sum_{i,j} |W_{ij}(\mathbf{r}_1,\mathbf{r}_2,\omega)|^2, \tag{1.46}$$

where $W_{ij}(\mathbf{r}_1,\mathbf{r}_2,\omega)$ are the elements of the cross-spectral density matrix. Eq. (1.46) is the basic formula that is used throughout this thesis.

1.4 Propagation of correlations

We next adress the fundamental question of how the coherence properties of a source influence the state of coherence of the field that it produces. The evolution of coherence functions on propagation can be described in a more rigorous fashion, as we now discuss. The field $V(\mathbf{r}, t)$ satisfies the wave equation, i.e.,

$$\left(\nabla^2 - \frac{1}{c^2}\frac{\partial^2}{\partial t^2}\right) V(\mathbf{r}, t) = 0, \tag{1.47}$$

where

$$\nabla^2 \equiv \frac{\partial^2}{\partial x^2} + \frac{\partial^2}{\partial y^2} + \frac{\partial^2}{\partial z^2} \tag{1.48}$$

denotes the Laplacian. If we now take the complex conjugate of this expression and multiply it with the field at another point $\mathbf{r}_2$ at time t_2, we get

$$\nabla_1^2 V^*(\mathbf{r}_1, t_1)V(\mathbf{r}_2, t_2) = \frac{1}{c^2}\frac{\partial^2}{\partial t_1^2} V^*(\mathbf{r}_1, t_1)V(\mathbf{r}_2, t_2). \tag{1.49}$$

Here the subscript 1 of the Laplacian indicates differentiation with respect to $\mathbf{r}_1$. We can take the ensemble average of both sides and interchange the order of differentiation and averaging to obtain

$$\nabla_1^2 \langle V^*(\mathbf{r}_1, t_1)V(\mathbf{r}_2, t_2)\rangle = \frac{1}{c^2}\frac{\partial^2}{\partial t_1^2} \langle V^*(\mathbf{r}_1, t_1)V(\mathbf{r}_2, t_2)\rangle. \tag{1.50}$$

If the field is statistically stationary, then

$$\langle V^*(\mathbf{r}_1, t_1)V(\mathbf{r}_2, t_2)\rangle = \Gamma(\mathbf{r}_1, \mathbf{r}_2, \tau), \tag{1.51}$$

with the time difference $\tau = t_2 - t_1$, and $\Gamma(\mathbf{r}_1, \mathbf{r}_2, \tau)$ the mutual coherence function. Clearly, $\partial^2/\partial t_1^2 = \partial^2/\partial\tau^2$. That means that we can re-write Eq. (1.50) as

$$\nabla_1^2 \Gamma(\mathbf{r}_1, \mathbf{r}_2, \tau) = \frac{1}{c^2}\frac{\partial^2}{\partial \tau^2}\Gamma(\mathbf{r}_1, \mathbf{r}_2, \tau). \tag{1.52}$$

This result shows that, just like the field itself, the mutual coherence function also satisfies the wave equation. Armed with this knowledge, we can calculate precisely how the correlation of a random optical field evolves on propagation through free space. Equation (1.52) is often applied in coherence theory to investigate the properties of the field that is generated by a source with a known (or prescribed) state of coherence.

By a completely similar approach as above, it can be derived that

$$\nabla_2^2 \Gamma(\mathbf{r}_1, \mathbf{r}_2, \tau) = \frac{1}{c^2} \frac{\partial^2}{\partial \tau^2} \Gamma(\mathbf{r}_1, \mathbf{r}_2, \tau). \tag{1.53}$$

In this equation the spatial differentiation is with respect to the variable $\mathbf{r}_2$, rather than $\mathbf{r}_1$.

After this discussion it will perhaps not come as a surprise that the cross-spectral density function, the space-frequency counterpart of the mutual coherence function, satisfies a pair of Helmholtz equations, namely

$$\left(\nabla_1^2 + k^2\right) W(\mathbf{r}_1, \mathbf{r}_2, \omega) \quad = 0, \tag{1.54}$$
$$\left(\nabla_2^2 + k^2\right) W(\mathbf{r}_1, \mathbf{r}_2, \omega) \quad = 0. \tag{1.55}$$

Together the four formulas (1.52)–(1.55) are known as the *Wolf equations*, after their discoverer Emil Wolf. It is fair to say that they form the basis of the modern theory of optical coherence. One way these expressions can be applied is to study how the correlation functions evolve on propagation from a source plane on which the state of coherence is known. To illustrate this, let us consider a random field $W^{(0)}(\mathbf{r}_1, \mathbf{r}_2, \omega)$ in a plane $z = 0$, that propagates into the half space $z > 0$. The solution of Eqs. (1.54) and (1.55) is

$$\begin{aligned} W(\boldsymbol{\rho}_1, \boldsymbol{\rho}_2, \omega, z) = \frac{1}{4\pi^2} & \iint W^{(0)}(\mathbf{r}_1, \mathbf{r}_2, \omega) \\ \times \frac{\partial}{\partial z} & \left(\frac{e^{-\mathrm{i}kR_1}}{R_1}\right) \frac{\partial}{\partial z} \left(\frac{e^{\mathrm{i}kR_2}}{R_2}\right) \mathrm{d}^2\mathbf{r}_1 \mathrm{d}^2\mathbf{r}_2, \end{aligned} \tag{1.56}$$

where $\boldsymbol{\rho}_1 = (u_1, v_1), \boldsymbol{\rho}_2 = (u_2, v_2), \mathbf{r}_1 = (x_1, y_1), \mathbf{r}_2 = (x_2, y_2)$ denote the transverse position vector in the z plane and the source plane, respectively. $R_1 = \sqrt{(\boldsymbol{\rho}_1 - \mathbf{r}_1)^2 + z^2}$, $R_2 = \sqrt{(\boldsymbol{\rho}_2 - \mathbf{r}_2)^2 + z^2}$ is the distance as showed

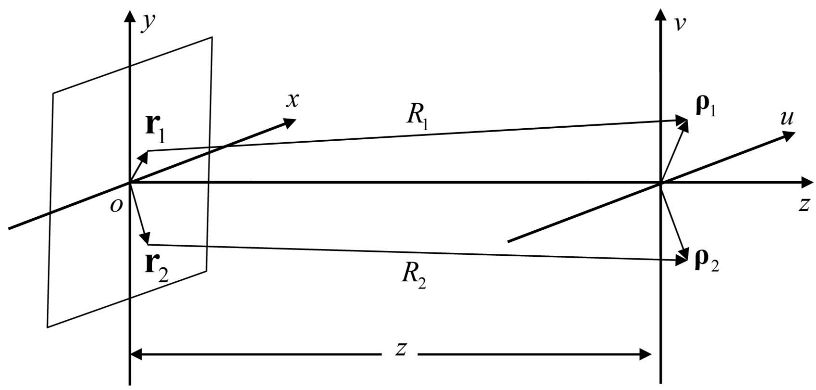

Figure 1.4: A schematic diagram of the propagation of a beam in paraxial approximation.

in Fig. (1.4). When $R_1, R_2 \gg \lambda$ is satisfied, Eq. (1.56) can be simplified to

$$W(\boldsymbol{\rho}_1, \boldsymbol{\rho}_2, \omega, z) = \left(\frac{z}{\lambda}\right)^2 \iint W^{(0)}(\mathbf{r}_1, \mathbf{r}_2, \omega) \times \left(\frac{e^{-\mathrm{i}kR_1}}{R_1^2}\right)\left(\frac{e^{\mathrm{i}kR_2}}{R_2^2}\right) \mathrm{d}^2\mathbf{r}_1 \mathrm{d}^2\mathbf{r}_2. \tag{1.57}$$

When the Fresnel approximation holds, i.e., $z \gg |u_1 - x_1|, |v_1 - y_1|$ and $z \gg |u_2 - x_2|, |v_2 - y_2|$, Eq. (1.57) can be written as

$$W(\boldsymbol{\rho}_1, \boldsymbol{\rho}_2, \omega, z) = \left(\frac{1}{\lambda z}\right)^2 \iint W^{(0)}(\mathbf{r}_1, \mathbf{r}_2, \omega) \times \exp\left[-\frac{\mathrm{i}k}{2z}(\boldsymbol{\rho}_1 - \mathbf{r}_1)^2\right] \exp\left[\frac{\mathrm{i}k}{2z}(\boldsymbol{\rho}_2 - \mathbf{r}_2)^2\right] \mathrm{d}^2\mathbf{r}_1 \mathrm{d}^2\mathbf{r}_2. \tag{1.58}$$

Eq. (1.58) is the propagation formula of the cross-spectral density function in free space that we frequently use in this thesis. In a similar way, the propagation formula for a stochastic electromagnetic beam can be expressed as

$$\mathbf{W}(\boldsymbol{\rho}_1, \boldsymbol{\rho}_2, \omega, z) = \left(\frac{1}{\lambda z}\right)^2 \iint \mathbf{W}^{(0)}(\mathbf{r}_1, \mathbf{r}_2, \omega) \times \exp\left[-\frac{\mathrm{i}k}{2z}(\boldsymbol{\rho}_1 - \mathbf{r}_1)^2\right] \exp\left[\frac{\mathrm{i}k}{2z}(\boldsymbol{\rho}_2 - \mathbf{r}_2)^2\right] \mathrm{d}^2\mathbf{r}_1 \mathrm{d}^2\mathbf{r}_2. \tag{1.59}$$

1.5 Outline of this thesis

This thesis is based upon four studies of the Hanbury Brown-Twiss effect in stochastic, electromagnetic beams. In Chapter 1 the necessary mathematical framework, the theory of optical coherence, is briefly reviewed.

Chapter 2 describes the radiation of a stochastic source, and how different correlations gradually build up as the field propagates. It is found that fourth-order correlations, such as the HBT effect, display a more complicated behavior than second-order correlations.

In Chapter 3 a special class of random sources is described, namely those of the quasi-homogeneous type. Roughly speaking, those are sources whose transverse spatial correlation length is much small than the source dimensions. Recently, reciprocity relations were derived for such sources. These relations describe the far-zone statistical properties of the field in terms of the source parameters. In this chapter we apply them to study the HBT effect. This leads to a new approach of an inverse problem: determining the source shape from HBT measurements in the far field. The HBT effect for a wide class of sources, so-called Gaussian Schell-model sources, are the subject of Chapter 4. Using both analytical and numerical tools, the influence of the state of polarization of the source on the upper limit of the correlations is charted.

The final Chapter, number 5, shows that the HBT effect is just one particular manifestation of a wider class of so-called Stokes fluctuation correlations. Also the classic notion of a scintillation coefficient can be generalized to what is termed a Stokes scintillation. It turns out that these generalized correlations and scintillations are not independent, but are related by sum rules. These results are illustrated for the case of a Gaussian Schell-model beam.

We end this thesis with a summary in Dutch of our results.

1.5.1 Publications

This thesis is based on the following publications:

- Gaofeng Wu and Taco D. Visser, "Hanbury Brown-Twiss effect with partially coherent electromagnetic beams," Optics Letters, vol. 39, pp. 2561–2564 (2014).
- Gaofeng Wu and Taco D. Visser, "Correlation of intensity fluctuations in beams generated by quasi-homogeneous sources," Journal of the Optical Society of America A, vol. 31, pp. 2152–2159 (2014).
- Xianlong Liu, Gaofeng Wu, Xiaoyan Pang, David Kuebel and Taco D. Visser, "Polarization and coherence in the Hanbury Brown-Twiss effect," Journal of Modern Optics, vol. 65, pp. 1437–1441 (2018).
- Gaofeng Wu, David Kuebel and Taco D. Visser, "A generalized Hanbury Brown-Twiss effect in partially coherent electromagnetic beams," Physical Review A, vol. 99, 033846 (2019).

Chapter 2

Hanbury Brown-Twiss effect with partially coherent electromagnetic beams

This Chapter is based on

- Gaofeng Wu and Taco D. Visser, "Hanbury Brown-Twiss effect with partially coherent electromagnetic beams," Optics Letters, vol. 39, 2561–2564 (2014).

Abstract
We derive expressions that allow us to examine the influence of different source parameters on the correlation of intensity fluctuations (the Hanbury Brown-Twiss effect) at two points in the same cross-section of a random electromagnetic beam. It is found that these higher-order correlations behave quite differently from the lower-order amplitude-phase correlations that are described by the spectral degree of coherence.

2.1 Introduction

Ever since Hanbury Brown and Twiss (HBT) determined the angular diameter of radio stars by analyzing the correlation of intensity fluctuations of their radiation [Hanbury Brown and Twiss, 1954; Hanbury Brown and Twiss, 1956], the eponymous "HBT effect" has been applied in many branches of physics [Baym, 1998; Schellekens *et al.*, 2005; Ottl *et al.*, 2005; Gutierrez, 2006; Glauber, 1963; Kuebel *et al.*, 2013]. In many cases a scalar analysis as given in [Wolf, 2007, Ch. 7] turns out to be sufficient. However, since the formulation of the unified theory of coherence and polarization [Wolf, 2003b; Wolf, 2003a; Roychowdhury and Wolf, 2003], several studies have been devoted to the question of how the HBT effect in random electromagnetic beams can be analyzed [Shirai and Wolf, 2007; Volkov *et al.*, 2008; Al-Qasimi *et al.*, 2010; Hassinen *et al.*, 2011; Li, 2014]. It is well known that the fundamental properties of these beams, such as their spectrum, degree of polarization, state of polarization and degree of coherence, can all change significantly on propagation, even when the propagation is through free space [James, 1994; Gori *et al.*, 1998; Gori *et al.*, 2001; Shirai and Wolf, 2004; Korotkova and Wolf, 2005; Raghunathan *et al.*, 2012; Raghunathan *et al.*, 2013]. However, until now a detailed investigation of the evolution of the HBT effect in random electromagnetic beams is lacking. In the present paper we intend to fill this void by examining the correlation of intensity fluctuations occurring in a wide class of partially coherent beams, namely those of the Gaussian Schell-model type [Gori *et al.*, 2001]. We derive expressions that allow us to examine the influence of different source parameters on the HBT effect at two points in the same cross-sectional plane.

2.2 Correlation of the intensity fluctuations

Let us consider a stochastic, wide-sense stationary, electromagnetic beam propagating close to the z direction into the half space $z > 0$ (see Fig. 2.1). The source plane is taken to be the plane $z = 0$. The vector $\boldsymbol{\rho} = (x, y)$ indicates a position in a transverse plane. Let $E_x(\boldsymbol{\rho}, z, \omega)$ and $E_y(\boldsymbol{\rho}, z, \omega)$ be the Cartesian components of the electric field at frequency ω along two mutually orthogonal x and y directions, perpendicular to the beam axis. The intensity of a single realization of the beam at a point $(\boldsymbol{\rho}, z)$ at frequency ω can be expressed as

$$I(\boldsymbol{\rho}, z, \omega) = |E_x(\boldsymbol{\rho}, z, \omega)|^2 + |E_y(\boldsymbol{\rho}, z, \omega)|^2. \tag{2.1}$$

From now on we will suppress the dependence on the frequency ω in our notation. The intensity $I(\boldsymbol{\rho}, z)$ is a random quantity and its variation from its mean value is

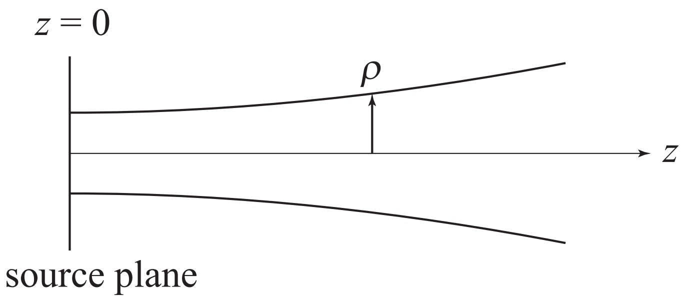

Figure 2.1: Illustrating the notation.

$$\Delta I(\boldsymbol{\rho}, z) = I(\boldsymbol{\rho}, z) - \langle I(\boldsymbol{\rho}, z)\rangle\,, \tag{2.2}$$

where the angular brackets denote the ensemble average. The statistical properties of the beam at a pair of points in a cross-section z are described by the electric cross-spectral density matrix $\mathbf{W}(\boldsymbol{\rho}_1, \boldsymbol{\rho}_2, z)$, whose elements are defined as

$$W_{ij}(\boldsymbol{\rho}_1, \boldsymbol{\rho}_2, z) = \langle E_i^*(\boldsymbol{\rho}_1, z) E_j(\boldsymbol{\rho}_2, z)\rangle\,, (i, j = x, y). \tag{2.3}$$

It follows from this definition that the ensemble-averaged intensity can be expressed as

$$\langle I(\boldsymbol{\rho}, z)\rangle = \mathrm{Tr}\,\mathbf{W}(\boldsymbol{\rho}, \boldsymbol{\rho}, z), \tag{2.4}$$

where Tr denotes the trace.
The correlation of the intensity fluctuations at two points $\boldsymbol{\rho}_1$ and $\boldsymbol{\rho}_2$ in the same cross-section z is defined as

$$C(\boldsymbol{\rho}_1, \boldsymbol{\rho}_2, z) = \langle \Delta I(\boldsymbol{\rho}_1, z)\Delta I(\boldsymbol{\rho}_2, z)\rangle\,. \tag{2.5}$$

We assume that the statistical properties of the beam are Gaussian. It then follows, by use of the Gaussian moment theorem for complex random processes, that the correlation of the intensity fluctuations at two positions may be expressed as [Mandel and Wolf, 1995, Ch. 8]

$$C(\boldsymbol{\rho}_1, \boldsymbol{\rho}_2, z) = \sum_{i,j} |W_{ij}(\boldsymbol{\rho}_1, \boldsymbol{\rho}_2, z)|^2. \tag{2.6}$$

2.3 Electromagnetic Gaussian Schell-model beams

We will study the correlation properties of a wide class of random beams, namely, those of the Gaussian Schell-model type [Gori *et al.*, 2001]. For these beams the elements of the cross-spectral density matrix in the source plane $z = 0$ read

$$W_{ij}(\boldsymbol{\rho}_1, \boldsymbol{\rho}_2, 0) = \sqrt{S_i(\boldsymbol{\rho}_1) S_j(\boldsymbol{\rho}_2)} \mu_{ij}(\boldsymbol{\rho}_2 - \boldsymbol{\rho}_1), \tag{2.7}$$

with the spectral densities $S_i(\boldsymbol{\rho}) = W_{ii}(\boldsymbol{\rho}, \boldsymbol{\rho})$ and the correlation coefficients $\mu_{ij}(\boldsymbol{\rho}_2 - \boldsymbol{\rho}_1)$ both Gaussian functions; i.e.,

$$S_i(\boldsymbol{\rho}) = A_i^2 \exp(-\rho^2/2\sigma_i^2), \tag{2.8}$$

$$\mu_{ij}(\boldsymbol{\rho}_2 - \boldsymbol{\rho}_1) = B_{ij} \exp[-(\boldsymbol{\rho}_2 - \boldsymbol{\rho}_1)^2/2\delta_{ij}^2]. \tag{2.9}$$

The parameters A_i, B_{ij}, σ_i and δ_{ij} are independent of position, but may depend on the frequency ω. They cannot be chosen arbitrarily. In particular, it follows from the definition of the cross-spectral density matrix that

$$B_{xx} = B_{yy} = 1, \tag{2.10}$$

$$B_{xy} = B_{yx}^*, \tag{2.11}$$

and

$$\delta_{xy} = \delta_{yx}. \tag{2.12}$$

In addition, the source parameters have to satisfy certain constraints to ensure that the field is beam-like at wavelength λ [KOROTKOVA *et al.*, 2004], and that the cross-spectral density matrix is positive definite, viz. [GORI *et al.*, 2008]

$$\frac{1}{4\sigma^2} + \frac{1}{\delta_{ii}^2} \ll \frac{2\pi^2}{\lambda^2}, \tag{2.13}$$

$$\sqrt{\frac{\delta_{xx}^2 + \delta_{yy}^2}{2}} \leq \delta_{xy} \leq \sqrt{\frac{\delta_{xx}\delta_{yy}}{|B_{xy}|}}, \tag{2.14}$$

and

$$|B_{xy}| \leq \frac{2}{\delta_{yy}/\delta_{xx} + \delta_{xx}/\delta_{yy}}. \tag{2.15}$$

If we take $\sigma_x = \sigma_y = \sigma$, then the matrix elements of the propagated beam in a plane z read (see [WOLF, 2007], where the one but the last minus sign of Eq. (10) on p. 184 should be a plus sign)

$$\begin{aligned} W_{ij}(\boldsymbol{\rho}_1, \boldsymbol{\rho}_2, z) = {} & \frac{A_i A_j B_{ij}}{\Delta_{ij}^2(z)} \exp\left[-\frac{(\boldsymbol{\rho}_1 + \boldsymbol{\rho}_2)^2}{8\sigma^2\Delta_{ij}^2(z)}\right] \\ & \times \exp\left[-\frac{(\boldsymbol{\rho}_1 - \boldsymbol{\rho}_2)^2}{2\Omega_{ij}^2\Delta_{ij}^2(z)} + \frac{\mathrm{i}k(\rho_2^2 - \rho_1^2)}{2R_{ij}(z)}\right], \end{aligned} \tag{2.16}$$

where

$$\Delta_{ij}^2(z) = 1 + (z/\sigma k \Omega_{ij})^2, \tag{2.17}$$

$$\frac{1}{\Omega_{ij}^2} = \frac{1}{4\sigma^2} + \frac{1}{\delta_{ij}^2}, \tag{2.18}$$

and

$$R_{ij}(z) = [1 + (\sigma k \Omega_{ij}/z)^2] z. \tag{2.19}$$

In the following we take the reference point $\boldsymbol{\rho}_1$ to be on the z axis, i.e., $\boldsymbol{\rho}_1 = 0$. On substituting from Eq. (2.16) into Eq. (2.6), we obtain the expression

$$
\begin{aligned}
C(0, \boldsymbol{\rho}_2, z) = \sum_{i,j} & \frac{A_i^2 A_j^2 |B_{ij}|^2}{\Delta_{ij}^4(z)} \\
& \times \exp\left[-\frac{\rho_2^2}{4\sigma^2 \Delta_{ij}^2(z)} - \frac{\rho_2^2}{\Omega_{ij}^2 \Delta_{ij}^2(z)}\right].
\end{aligned}
\tag{2.20}
$$

Notice that Eq. (2.20) implies that $C(0, \boldsymbol{\rho}_2, z)$ is rotationally symmetric about the z axis, i.e., it only depends on $\rho_2 = |\boldsymbol{\rho}_2|$. We define the normalized correlation function as

$$
C_N(0, \boldsymbol{\rho}_2, z) = \frac{C(0, \boldsymbol{\rho}_2, z)}{\langle I(0, z)\rangle \langle I(\boldsymbol{\rho}_2, z)\rangle},
\tag{2.21}
$$

where

$$
\langle I(0, z)\rangle = \frac{A_x^2}{\Delta_{xx}^2(z)} + \frac{A_y^2}{\Delta_{yy}^2(z)},
\tag{2.22}
$$

and

$$
\begin{aligned}
\langle I(\rho_2, z)\rangle = & \frac{A_x^2}{\Delta_{xx}^2(z)} \exp\left[-\frac{\rho_2^2}{2\sigma^2 \Delta_{xx}^2(z)}\right] \\
& + \frac{A_y^2}{\Delta_{yy}^2(z)} \exp\left[-\frac{\rho_2^2}{2\sigma^2 \Delta_{yy}^2(z)}\right].
\end{aligned}
\tag{2.23}
$$

It can be shown that $C_N(0, \boldsymbol{\rho}_2, z)$ is bounded by zero and unity [Hassinen *et al.*, 2011]. It is easily derived that

$$
\lim_{z\to\infty} C_N(0, \boldsymbol{\rho}_2, z) = \frac{\sum\limits_{i,j} A_i^2 A_j^2 |B_{ij}|^2 \Omega_{ij}^4}{\left(A_x^2 \Omega_{xx}^2 + A_y^2 \Omega_{yy}^2\right)^2}.
\tag{2.24}
$$

Notice that this asymptotic value is independent of the choice of the point $\boldsymbol{\rho}_2$. Eq. (2.24) is generally valid, in contrast to the much more restricted analysis presented in [Li, 2014]. We will compare the fourth-order correlation function $C_N(0, \boldsymbol{\rho}_2, z)$ with the second-order spectral degree of coherence. The latter is defined as [Wolf, 2007, Sec. 9.2]

$$
\eta(0, \boldsymbol{\rho}_2, z) = \frac{\mathrm{Tr}\ \mathbf{W}(0, \boldsymbol{\rho}_2, z)}{\sqrt{\langle I(0, z)\rangle}\sqrt{\langle I(\boldsymbol{\rho}_2, z)\rangle}},
\tag{2.25}
$$

and is a direct measure of the visibility of the fringe pattern produced in Young's experiment. Note that, in contrast to Eq. (2.24),

$$\lim_{z\to\infty} \eta(0, \boldsymbol{\rho}_2, z) = 1. \tag{2.26}$$

We now employ the above theoretical development to study the evolution of the second- and fourth-order correlations of a GSM beam on propagation in free space. In the examples we set $\lambda = 0.6328\ \mu$m, $\sigma = 4$ mm, $A_x = 1$, $A_y = 3$, $|B_{xy}| = 0.2$, $\delta_{xx} = 3$ mm, $\delta_{xy} = 2.7$ mm and $\delta_{yy} = 1$ mm, unless specified otherwise. For these values, the conditions (2.13)–(2.15) are all satisfied. A comparison of the contours of $C_N(0, \boldsymbol{\rho}_2, z)$ and those of $|\eta(0, \rho_2, z)|$ in the $z\rho_2$-plane (Figs. 2.2 and 2.3) indicates that the evolution of the correlation of intensity fluctuations is more complicated than that of the spectral degree of coherence. This is further illustrated by Fig. 2.4 from which it is seen that $|\eta(0, \rho_2, z)|$ increases monotonically to the value 1, whereas $C_N(0, \boldsymbol{\rho}_2, z)$ quickly rises to its maximum value, then decreases, after which it slowly rises to its asymptotic limit.

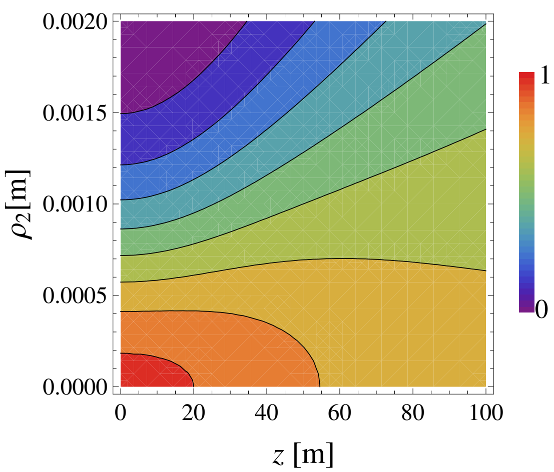

Figure 2.2: Contours of the normalized correlation of intensity fluctuations $C_N(0, \boldsymbol{\rho}_2, z)$ in the $z\rho_2$ plane.

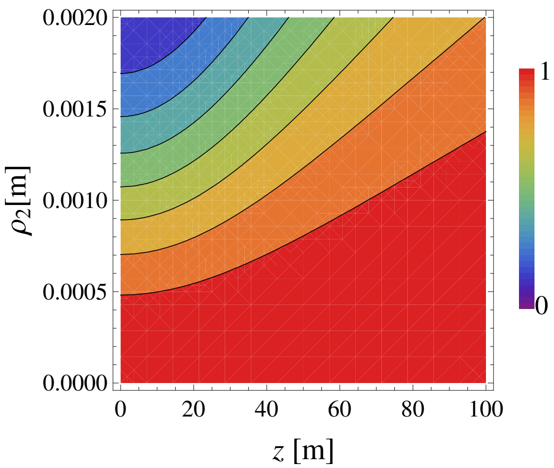

Figure 2.3: Contours of the modulus of the spectral degree of coherence $|\eta(0, \rho_2, z)|$ in the $z\rho_2$ plane.

An essential difference between the spectral degree of coherence and the correlation of intensity fluctuations is that $\eta(0, \rho_2, z)$ only depends on the diagonal elements of the cross-spectral density matrix, whereas the definition of $C_N(0, \boldsymbol{\rho}_2, z)$ contains all four matrix elements. A direct consequence is that the spectral degree of coherence is unaffected by changes in the coherence length δ_{xy}. The correlation of intensity fluctuations, on the other hand, is quite sensitive to changes in this parameter, as is shown in Fig. 2.5. The influence of the coherence length δ_{xx} at a fixed point in the beam is shown in Fig. 2.6. It is seen that $|\eta(0, \rho_2, z)|$ is less sensitive than $C_N(0, \boldsymbol{\rho}_2, z)$. A similar result is obtained when the amplitude A_y is varied. This is illustrated in Fig. 2.7.

We noted before that the asymptotic value of $C_N(0, \boldsymbol{\rho}_2, z)$ is independent of the choice of the point ρ_2. In Fig. 2.8(a) the variation of the correlation of intensity fluctuations is plotted for several values of ρ_2. Although these curves are quite distinct as $z < 100$ m, they eventually all approach the limiting value indicated by the dashed line. For comparison's sake the evolution of $|\eta(0, \rho_2, z)|$ is shown in Fig. 2.8(b).

It is interesting to note that expression Eq. (2.24) offers several options

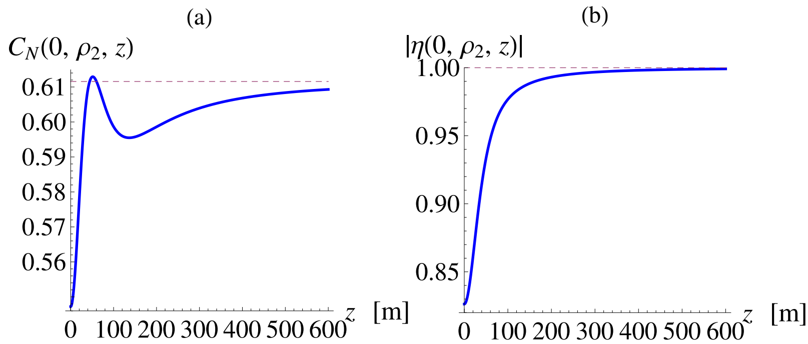

Figure 2.4: Evolution of (a) the normalized correlation of intensity fluctuations, and (b) the modulus of the spectral degree of coherence for the choice $\rho_2 = 0.65$ mm. The dashed lines are the asymptotic values given by Eqs. (2.24) and (2.26), respectively.

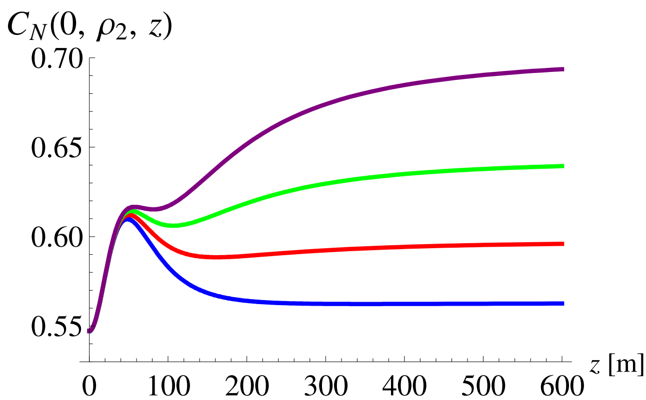

Figure 2.5: Evolution of the normalized correlation of intensity fluctuations as a function of z for different values of the parameter δ_{xy} with $\rho_2 = 0.65$ mm. . From bottom to top: $\delta_{xy} = 2.3$ mm (blue), 2.6 mm (red), 2.9 mm (green), 3.2 mm (purple).

to tailor the correlation of the intensity fluctuations in the far-field. One possibility is to change the ratio of the two spectral densities A_x and A_y. It immediately follows from Eq. (2.24) that $\lim_{z\to\infty} C_N(0, \boldsymbol{\rho}_2, z) = 1$ if one of

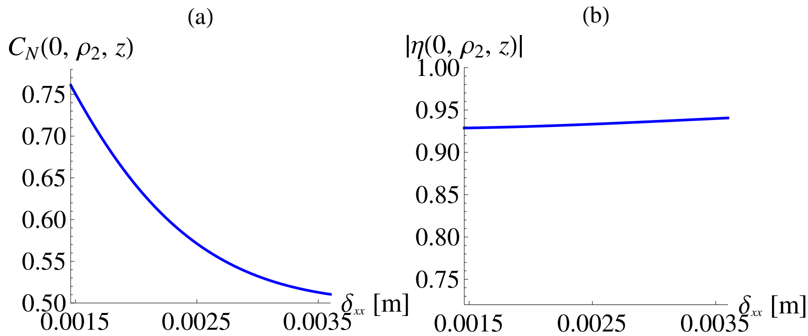

Figure 2.6: Variation of (a) the normalized correlation of intensity fluctuations and (b) the modulus of the spectral degree of coherence as a function of δ_{xx} at the point $\rho_2 = 2$ mm, $z = 200$ m.

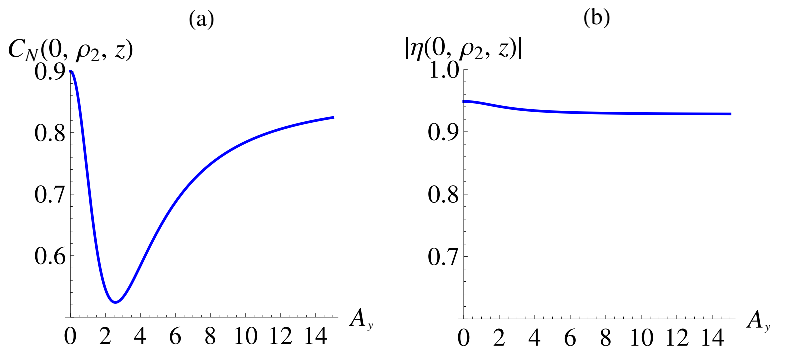

Figure 2.7: Variation of (a) the normalized correlation of intensity fluctuations and (b) the modulus of the spectral degree of coherence as a function of A_y at the point $\rho_2 = 2$ mm, $z = 200$ m.

the spectral densities is zero, i.e. if the beam is linearly polarized. As is seen from Fig. 2.9, the asymptotic value of $C_N(0, \boldsymbol{\rho}_2, z)$ can be varied from its maximum value of 1 down to a value of 0.5. In this example $\sigma = 1$ mm, $|B_{xy}| = 0.1$, $\delta_{xx} = 3$ mm, $\delta_{xy} = 2.5$ mm and $\delta_{yy} = 3$ mm .

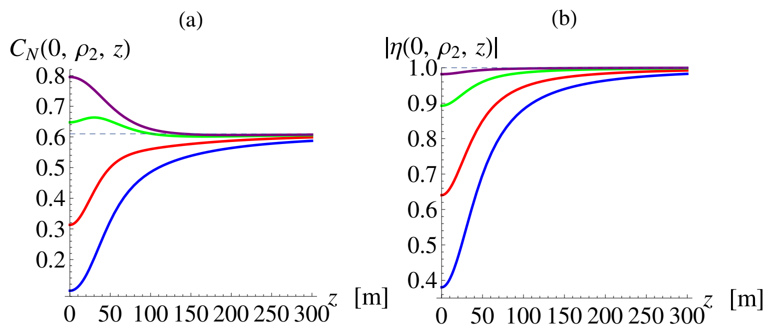

Figure 2.8: Evolution of (a) the normalized correlation of intensity fluctuations and (b) the modulus of the spectral degree of coherence for different choices of ρ_2. From bottom to top : $\rho_2 = 1.5$ mm (blue), 1 mm (red), 0.5 mm (green), 0.2 mm (purple), the dashed lines are the asymptotic value given by Eq. (24) and Eq. (26), respectively.

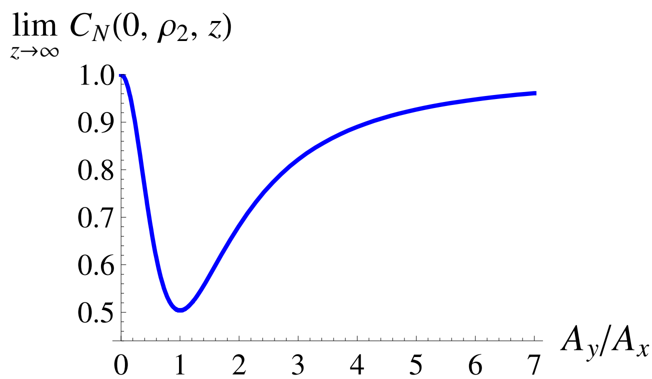

Figure 2.9: Variation of the far-zone value of $C_N(0, \boldsymbol{\rho}_2, z)$ as a function of the ratio A_y/A_x.

2.4 Conclusions

In conclusion, we have studied the evolution of the Hanbury Brown-Twiss effect on propagation of a electromagnetic Gaussian Schell-model beam. The influence of the different source parameters was explored numerically. It was found that the correlation of intensity fluctuations in the far-field can be tuned by adjusting, for example, the ratio of the amplitudes of the two components of the electric field.

Chapter 3

Correlation of intensity fluctuations in beams generated by quasi-homogeneous sources

This Chapter is based on

- Gaofeng Wu and Taco D. Visser, "Correlation of intensity fluctuations in beams generated by quasi-homogeneous sources," Journal of the Optical Society of America A, vol. 31, pp. 2152–2159 (2014).

Abstract
We derive expressions for the far-zone correlation of intensity fluctuations (the Hanbury Brown-Twiss effect) that occurs in electromagnetic beams that are generated by quasi-homogeneous sources. Such sources often have a radiant intensity pattern that is rotationally symmetric, irrespective of the source shape. We demonstrate how from the far-zone correlation of intensity fluctuations the spectral density distribution across the source plane may be reconstructed.

3.1 Introduction

In the mid 1950s Hanbury Brown and Twiss (HBT) determined the angular diameter of radio stars by analyzing their correlation of intensity fluctuations [Hanbury Brown and Twiss, 1954; Hanbury Brown and Twiss, 1956]. Since then such correlation measurements have proven to be a powerful tool that can be applied across all branches of physics, see for example, [Baym, 1998; Ottl *et al.*, 2005; Schellekens *et al.*, 2005; Kuebel *et al.*, 2013]. The original description of the HBT effect, which assumes a scalar wave field and is described in [Wolf, 2007, Ch. 7], was later generalized to electromagnetic beams, see [Mandel and Wolf, 1995, Ch. 8] and [Shirai and Wolf, 2007; Volkov *et al.*, 2008; Al-Qasimi *et al.*, 2010; Hassinen *et al.*, 2011]. One major class of partially coherent electromagnetic beams are those generated by so-called Gaussian Schell-model sources [Gori *et al.*, 2001]. Quite recently two studies were dedicated to the occurrence of the HBT effect in beams of this type [Li, 2014; Wu and Visser, 2014b]. Another important class of partially coherent sources, which partially overlaps with those of the Gaussian Schell-model type, is formed by quasi-homogeneous sources. In the space-frequency domain, scalar, secondary, planar quasi-homogeneous sources are characterized by a correlation function, the so-called spectral degree of coherence $\mu^{(0)}(\boldsymbol{\rho}_1, \boldsymbol{\rho}_2, \omega)$ that, at each frequency ω, depends on the source points $\boldsymbol{\rho}_1$ and $\boldsymbol{\rho}_2$ only through their difference $\boldsymbol{\rho}_2 - \boldsymbol{\rho}_1$, see Fig. 3.1. In addition, these sources have a spectral density $S^{(0)}(\boldsymbol{\rho}, \omega)$ that varies much slower with $\boldsymbol{\rho}$ than the modulus of the spectral degree of coherence varies with $\boldsymbol{\rho}_2 - \boldsymbol{\rho}_1$. The properties of quasi-homogeneous sources and those of the far-zone fields they generate, are related by two reciprocity relations. One connects the spectral density of the far field to the spatial Fourier transform of the spectral degree of coherence in the source plane. The other connects the far-zone spectral degree of coherence to the spatial Fourier transform of the spectral density of the source [Collett and Wolf, 1980; Li and Wolf, 1982; Wolf and Carter, 1984; Carter and Wolf, 1985; Kim and Wolf, 1987; Foley and Wolf, 1995; Carter and Wolf, 1997; Visser *et al.*, 2006]. Quite recently, the notion of quasi-homogeneity has been extended to electromagnetic sources, and reciprocity relations have been derived for the beams that they generate [Raghunathan *et al.*, 2013]. These relations were then used to illustrate how fundamental field properties such as its spectrum, polarization and state of coherence in the far zone typically differ from those in the source plane. In the present paper we apply these novel reciprocity relations, under the assumption of Gaussian statistics, to study the HBT effect. We derive general expressions for the correlation of intensity fluctuations of the far-zone field, and illustrate our results with several examples. Quasi-homogeneous sources can produce a radiant intensity that is rotationally symmetric, even when the source distribution lacks any symmetry. We demonstrate that the HBT correlations, in contrast to the radiant intensity, provide information about the source shape. For example, in certain cases the aspect ratio of the source can be recovered. Since HBT correlations are obtained from intensity measurements, rather than phase measurements, this provides a reconstruction scheme that is relatively robust to signal degrading factors such as turbulence.

3.2 Correlation of intensity fluctuations of partially coherent electromagnetic beams

Let us consider a stochastic, wide-sense stationary, electromagnetic beam propagating close to the z direction into the half space $z > 0$ (see Fig. 3.1). The source is taken to be the plane $z = 0$. The vector $\boldsymbol{\rho} = (x, y)$ denotes a position in a transverse plane. Let $E_x(\boldsymbol{\rho}, z, \omega)$ and $E_y(\boldsymbol{\rho}, z, \omega)$ be the Cartesian components of the electric field at frequency ω along two mutually orthogonal x and y directions, perpendicular to the beam axis. The intensity of a single realization of the beam at a point $(\boldsymbol{\rho}, z)$ at frequency ω can be expressed as

$$I(\boldsymbol{\rho}, z, \omega) = |E_x(\boldsymbol{\rho}, z, \omega)|^2 + |E_y(\boldsymbol{\rho}, z, \omega)|^2. \tag{3.1}$$

From now on we suppress the dependence on the frequency ω in our notation. The intensity is a random quantity, and its variation from its mean value is

$$\Delta I(\boldsymbol{\rho}, z) = I(\boldsymbol{\rho}, z) - \langle I(\boldsymbol{\rho}, z)\rangle\,, \tag{3.2}$$

where the angular brackets denote an ensemble average. The statistical properties of such a beam at a pair of points in a cross-sectional plane z

are described by the 2 × 2 cross-spectral density matrix which is defined as [Wolf, 2003b]

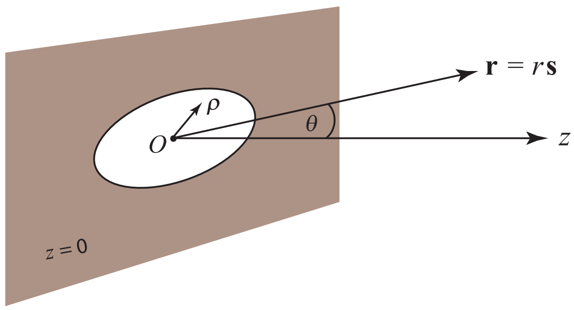

Figure 3.1: Illustrating the notation. The origin O of a right-handed Cartesian coordinate system is taken in the source plane $z = 0$. The transverse two-dimensional vector $\boldsymbol{\rho} = (x, y)$ indicates the position of a source point. The position vector $\mathbf{r}$ of a point in the far zone makes an angle θ with the positive z axis. Also, $r = |\mathbf{r}|$, and $\mathbf{s}$ is a directional unit vector.

$$\mathbf{W}(\boldsymbol{\rho}_1, \boldsymbol{\rho}_2, z) = \begin{bmatrix} W_{xx}(\boldsymbol{\rho}_1, \boldsymbol{\rho}_2, z) & W_{xy}(\boldsymbol{\rho}_1, \boldsymbol{\rho}_2, z) \\ W_{yx}(\boldsymbol{\rho}_1, \boldsymbol{\rho}_2, z) & W_{yy}(\boldsymbol{\rho}_1, \boldsymbol{\rho}_2, z) \end{bmatrix}. \tag{3.3}$$

It follows from this definition that the ensemble-averaged intensity can be expressed as

$$\langle I(\boldsymbol{\rho}, z)\rangle = \mathrm{Tr}\,\mathbf{W}(\boldsymbol{\rho}, \boldsymbol{\rho}, z), \tag{3.4}$$

where Tr denotes the trace. The correlation of intensity fluctuations at points $\boldsymbol{\rho}_1$ and $\boldsymbol{\rho}_2$ in the same cross-sectional plane z is defined as

$$C(\boldsymbol{\rho}_1, \boldsymbol{\rho}_2, z) = \langle \Delta I(\boldsymbol{\rho}_1, z)\Delta I(\boldsymbol{\rho}_2, z)\rangle \,. \tag{3.5}$$

We assume that the random fluctuations of the source are governed by a Gaussian process. It then follows, by use of the Gaussian moment theorem, that the correlation of intensity fluctuations may be expressed in terms of elements of the cross-spectral density matrix as [Mandel and Wolf, 1995, Ch. 8]

$$C(\boldsymbol{\rho}_1, \boldsymbol{\rho}_2, z) = \sum_{i,j} |W_{ij}(\boldsymbol{\rho}_1, \boldsymbol{\rho}_2, z)|^2, \quad (i, j = x, y). \tag{3.6}$$

3.3 Quasi-homogeneous, secondary planar electromagnetic sources

In this section we establish our notation and briefly review some recently derived reciprocity relations.

The elements of the cross-spectral density matrix in the source plane can be written in the form [Wolf, 2007, Ch. 9.4.2]

$$W_{ij}^{(0)}(\boldsymbol{\rho}_1, \boldsymbol{\rho}_2) = \sqrt{S_i^{(0)}(\boldsymbol{\rho}_1) S_j^{(0)}(\boldsymbol{\rho}_2)}\, \mu_{ij}^{(0)}(\boldsymbol{\rho}_2 - \boldsymbol{\rho}_1), \quad (i, j = x, y) \tag{3.7}$$

where $S_i^{(0)}(\boldsymbol{\rho}) = \langle |E_i(\boldsymbol{\rho})|^2 \rangle$ denotes the spectral density associated with the Cartesian component E_i of the electric field vector in the plane $z = 0$. Its two-dimensional spatial Fourier transform is defined as

$$\tilde{S}_i^{(0)}(\mathbf{f}) = \frac{1}{(2\pi)^2} \int_{z=0} S_i^{(0)}(\boldsymbol{\rho}) \exp(-\mathrm{i}\mathbf{f} \cdot \boldsymbol{\rho})\, d^2\rho. \tag{3.8}$$

We also introduce the function

$$S_{xy}^{(0)}(\boldsymbol{\rho}) = \sqrt{S_x^{(0)}(\boldsymbol{\rho})} \sqrt{S_y^{(0)}(\boldsymbol{\rho})}, \tag{3.9}$$

and its Fourier transform

$$\tilde{S}_{xy}^{(0)}(\mathbf{f}) = \frac{1}{(2\pi)^2} \int_{z=0} \sqrt{S_x{}^{(0)}(\boldsymbol{\rho})} \sqrt{S_y{}^{(0)}(\boldsymbol{\rho})} \exp(-\mathrm{i}\mathbf{f} \cdot \boldsymbol{\rho})\, d^2\rho. \tag{3.10}$$

Similarly, the spatial Fourier transform of the four correlation coefficients $\mu_{ij}^{(0)}(\boldsymbol{\rho})$ is given by the expression

$$\tilde{\mu}_{ij}^{(0)}(\mathbf{f}) = \frac{1}{(2\pi)^2} \int_{z=0} \mu_{ij}^{(0)}(\boldsymbol{\rho}) \exp(-\mathrm{i}\mathbf{f} \cdot \boldsymbol{\rho})\, d^2\rho. \tag{3.11}$$

In Ref. [Raghunathan *et al.*, 2013] it was derived that for a planar, secondary quasi-homogenous source, the elements of the cross-spectral density matrix in the far zone, labeled by the superscript (∞), are connected to the source properties, labeled by the superscript (0), through the reciprocity relations

$$\begin{aligned} W_{xx}^{(\infty)}(r_1\mathbf{s}_1, r_2\mathbf{s}_2) = (2\pi k)^2 \cos\theta_1 \cos\theta_2 \frac{e^{\mathrm{i}k(r_2 - r_1)}}{r_2 r_1} \\ \times \tilde{S}_x^{(0)}[k(\mathbf{s}_{2\perp} - \mathbf{s}_{1\perp})]\, \tilde{\mu}_{xx}^{(0)}[k(\mathbf{s}_{2\perp} + \mathbf{s}_{1\perp})/2], \end{aligned} \tag{3.12}$$

$$W_{xy}^{(\infty)}(r_1\mathbf{s}_1, r_2\mathbf{s}_2) = (2\pi k)^2 \cos\theta_1 \cos\theta_2 \frac{e^{ik(r_2-r_1)}}{r_2 r_1} \times \tilde{S}_{xy}^{(0)}[k(\mathbf{s}_{2\perp} - \mathbf{s}_{1\perp})]\, \tilde{\mu}_{xy}^{(0)}[k(\mathbf{s}_{2\perp} + \mathbf{s}_{1\perp})/2], \qquad (3.13)$$

$$W_{yx}^{(\infty)}(r_1\mathbf{s}_1, r_2\mathbf{s}_2) = (2\pi k)^2 \cos\theta_1 \cos\theta_2 \frac{e^{ik(r_2-r_1)}}{r_2 r_1} \times \tilde{S}_{xy}^{(0)}[k(\mathbf{s}_{2\perp} - \mathbf{s}_{1\perp})]\, \tilde{\mu}_{xy}^{(0)*}[k(\mathbf{s}_{2\perp} + \mathbf{s}_{1\perp})/2], \qquad (3.14)$$

$$W_{yy}^{(\infty)}(r_1\mathbf{s}_1, r_2\mathbf{s}_2) = (2\pi k)^2 \cos\theta_1 \cos\theta_2 \frac{e^{ik(r_2-r_1)}}{r_2 r_1} \times \tilde{S}_{y}^{(0)}[k(\mathbf{s}_{2\perp} - \mathbf{s}_{1\perp})]\, \tilde{\mu}_{yy}^{(0)}[k(\mathbf{s}_{2\perp} + \mathbf{s}_{1\perp})/2], \qquad (3.15)$$

where $k = 2\pi/\lambda$ is the wave number associated with wavelength λ, and $\mathbf{s}_{\alpha\perp} = (\sin\theta_\alpha \cos\phi_\alpha, \sin\theta_\alpha \sin\phi_\alpha)$ is the two-dimensional projection of the directional unit vector $\mathbf{s}_\alpha$ onto the xy-plane ($\alpha = 1, 2$). Furthermore, θ_α is the angle between $\mathbf{s}_\alpha$ and the positive z axis, and ϕ_α is the azimuthal angle in the xy plane.

The radiant intensity of the beam is defined as [Mandel and Wolf, 1995, Sec. 5.2]

$$\begin{aligned} J(r\mathbf{s}) &= r^2\, \mathrm{Tr}\, \mathbf{W}^{(\infty)}(r\mathbf{s}, r\mathbf{s}), \\ &= (2\pi k \cos\theta)^2 \left[\tilde{S}_x^{(0)}(0)\, \tilde{\mu}_{xx}^{(0)}(k\mathbf{s}_\perp) + \tilde{S}_y^{(0)}(0)\, \tilde{\mu}_{yy}^{(0)}(k\mathbf{s}_\perp)\right]. \end{aligned} \qquad (3.16)$$

It is seen from Eq. (3.16) that *if the functions $\tilde{\mu}_{xx}^{(0)}(k\mathbf{s}_\perp)$ and $\tilde{\mu}_{yy}^{(0)}(k\mathbf{s}_\perp)$ are both rotationally symmetric, i.e. if they only depend on $|k\mathbf{s}_\perp|$, than the radiant intensity is rotationally symmetric about the normal to the source plane, irrespective of the spectral density distribution of the source.* As we will see in Section 3.6, it is possible to construct sources whose radiant intensities have rotational symmetry, but whose correlation of intensity fluctuations lack such symmetry.

3.4 Beam conditions for quasi-homogeneous sources

In order that the field generated by a quasi-homogeneous source is beam-like, the radiant intensity $J(r\mathbf{s})$ must be negligible except when the unit vector $\mathbf{s}$ lies in a narrow solid angle about the z axis. It follows from Eq. (3.16) that this will be the case when both

$$|\tilde{\mu}_{xx}^{(0)}(k\mathbf{s}_\perp)| \approx 0, \tag{3.17}$$

$$|\tilde{\mu}_{yy}^{(0)}(k\mathbf{s}_\perp)| \approx 0, \tag{3.18}$$

unless $s_\perp^2 \ll 1$. To illustrate these two conditions, we consider a quasi-homogeneous source whose diagonal correlation coefficients are both Gaussian, i.e.

$$\mu_{xx}^{(0)}(\boldsymbol{\rho}) = \exp\left(-\frac{\rho^2}{2\delta_{xx}^2}\right), \tag{3.19}$$

$$\mu_{yy}^{(0)}(\boldsymbol{\rho}) = \exp\left(-\frac{\rho^2}{2\delta_{yy}^2}\right). \tag{3.20}$$

In that case

$$\tilde{\mu}_{xx}^{(0)}(k\mathbf{s}_\perp) = \frac{\delta_{xx}^2}{2\pi}\exp\left(-\frac{\delta_{xx}^2 k^2 s_\perp^2}{2}\right), \tag{3.21}$$

$$\tilde{\mu}_{yy}^{(0)}(k\mathbf{s}_\perp) = \frac{\delta_{yy}^2}{2\pi}\exp\left(-\frac{\delta_{yy}^2 k^2 s_\perp^2}{2}\right). \tag{3.22}$$

Eqs. (3.17) and (3.18) are clearly satisfied if both

$$\delta_{xx} \gg \frac{\lambda}{\pi\sqrt{2}}, \tag{3.23}$$

$$\delta_{yy} \gg \frac{\lambda}{\pi\sqrt{2}}. \tag{3.24}$$

These two beam conditions are a generalization of the result for scalar fields that was derived in [Mandel and Wolf, 1995, Sec. 5.6.4].

3.5 Correlation of intensity fluctuations

On substituting from Eqs. (3.12)–(3.15) into Eq. (3.6), we obtain for the correlation of intensity fluctuations in the far-zone the expression

$$
\begin{aligned}
C^{(\infty)}(r_1\mathbf{s}_1, r_2\mathbf{s}_2) = {} & \left[\frac{(2\pi k)^2\cos\theta_1\cos\theta_2}{r_1 r_2}\right]^2 \\
& \times\left\{\left|\tilde{S}_x^{(0)}[k(\mathbf{s}_{2\perp}-\mathbf{s}_{1\perp})]\tilde{\mu}_{xx}^{(0)}[k(\mathbf{s}_{2\perp}+\mathbf{s}_{1\perp})/2]\right|^2\right. \\
& + 2\left|\tilde{S}_{xy}^{(0)}[k(\mathbf{s}_{2\perp}-\mathbf{s}_{1\perp})]\tilde{\mu}_{xy}^{(0)}[k(\mathbf{s}_{2\perp}+\mathbf{s}_{1\perp})/2]\right|^2 \\
& \left. + \left|\tilde{S}_y^{(0)}[k(\mathbf{s}_{2\perp}-\mathbf{s}_{1\perp})]\tilde{\mu}_{yy}^{(0)}[k(\mathbf{s}_{2\perp}+\mathbf{s}_{1\perp})/2]\right|^2\right\}.
\end{aligned}
\tag{3.25}
$$

We introduce a normalized correlation of intensity fluctuations, labeled by the subscript N, by defining

$$
C_N^{(\infty)}(r_1\mathbf{s}_1, r_2\mathbf{s}_2) = \frac{C^{(\infty)}(r_1\mathbf{s}_1, r_2\mathbf{s}_2)}{\left\langle I^{(\infty)}(r_1\mathbf{s}_1)\right\rangle\left\langle I^{(\infty)}(r_2\mathbf{s}_2)\right\rangle}, \tag{3.26}
$$

where

$$
\begin{aligned}
\langle I^{(\infty)}(r_\alpha\mathbf{s}_\alpha)\rangle &= \mathrm{Tr}\,\mathbf{W}^{(\infty)}(r_\alpha\mathbf{s}_\alpha, r_\alpha\mathbf{s}_\alpha) \\
&= \left(\frac{2\pi k\cos\theta_\alpha}{r_\alpha}\right)^2\left[\tilde{S}_x^{(0)}(0)\,\tilde{\mu}_{xx}^{(0)}(k\mathbf{s}_{\alpha\perp}) + \tilde{S}_y^{(0)}(0)\,\tilde{\mu}_{yy}^{(0)}(k\mathbf{s}_{\alpha\perp})\right], \\
&\quad (\alpha = 1, 2).
\end{aligned}
\tag{3.27}
$$

From now on we consider pairs of observation points that are located symmetrically with respect to the z axis (see Fig. 3.2), i.e., we set $r_1 = r_2 = r$; $\mathbf{s}_{1\perp} = -\mathbf{s}_{2\perp} = -\mathbf{s}_\perp$, and $\theta_1 = \theta_2 = \theta$.

Since the four correlation coefficients $\mu_{ij}^{(0)}$ are "fast" functions of their argument, their Fourier transforms $\tilde{\mu}_{ij}^{(0)}$ will be "slow" functions. Hence we may write

$$
\tilde{\mu}_{ij}^{(0)}(k\mathbf{s}_{1\perp}) \approx \tilde{\mu}_{ij}^{(0)}(k\mathbf{s}_{2\perp}) \approx \tilde{\mu}_{ij}^{(0)}\left[\frac{k(\mathbf{s}_{2\perp}+\mathbf{s}_{1\perp})}{2}\right] = \tilde{\mu}_{ij}^{(0)}(0). \tag{3.28}
$$

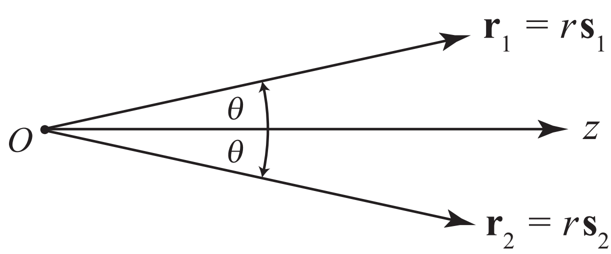

Figure 3.2: Two far-zone observation points $\mathbf{r}_1$ and $\mathbf{r}_2$ that are symmetrically located with respect to the z axis.

On making use of these approximations in Eq. (3.26), we find for the normalized correlation of the intensity fluctuations the formula

$$\begin{aligned} C_N^{(\infty)}(r\mathbf{s}_1, r\mathbf{s}_2) = & \left\{ \left| \tilde{S}_x^{(0)}(2k\mathbf{s}_\perp)\tilde{\mu}_{xx}^{(0)}(0) \right|^2 + 2\left| \tilde{S}_{xy}^{(0)}(2k\mathbf{s}_\perp)\tilde{\mu}_{xy}^{(0)}(0) \right|^2 \right. \\ & \left. + \left| \tilde{S}_y^{(0)}(2k\mathbf{s}_\perp)\tilde{\mu}_{yy}^{(0)}(0) \right|^2 \right\} \\ & \times \left[\tilde{S}_x^{(0)}(0)\tilde{\mu}_{xx}^{(0)}(0) + \tilde{S}_y^{(0)}(0)\tilde{\mu}_{yy}^{(0)}(0) \right]^{-2}, \\ & (r_1 = r_2 = r;\ \mathbf{s}_{1\perp} = -\mathbf{s}_{2\perp} = -\mathbf{s}_\perp). \end{aligned} \tag{3.29}$$

We will employ Eq. (3.29) to investigate the Hanbury Brown-Twiss effect for different kinds of sources.

3.6 Examples

Let us first consider an unpolarized, quasi-homogeneous source with an arbitrary shape. In that case we have

$$S_x^{(0)}(\boldsymbol{\rho}) = S_y^{(0)}(\boldsymbol{\rho}) = S^{(0)}(\boldsymbol{\rho}), \tag{3.30}$$

$$\mu_{xy}^{(0)}(\boldsymbol{\rho}) = 0. \tag{3.31}$$

We note that for an unpolarized source it is not necessary to have $\mu_{xx}^{(0)}(\boldsymbol{\rho}) = \mu_{yy}^{(0)}(\boldsymbol{\rho})$, see also the discussion in [Visser *et al.*, 2009]. Substitution from

Eqs. (3.30) and (3.31) into Eq. (3.29) yields the expression

$$C_N^{(\infty)}(r\mathbf{s}_1, r\mathbf{s}_2) = \frac{\left|\tilde{\mu}_{xx}^{(0)}(0)\right|^2 + \left|\tilde{\mu}_{yy}^{(0)}(0)\right|^2}{\left[\tilde{S}^{(0)}(0)\right]^2 \left[\tilde{\mu}_{xx}^{(0)}(0) + \tilde{\mu}_{yy}^{(0)}(0)\right]^2} |\tilde{S}^{(0)}(2k\mathbf{s}_\perp)|^2. \quad (3.32)$$

This result shows that for any planar, secondary quasi-homogeneous, unpolarized source the normalized correlation of intensity fluctuations between two symmetrically located far-zone points is proportional to $|\tilde{S}^{(0)}(2k\mathbf{s}_\perp)|^2$*, i.e., to the squared modulus of the Fourier transform of the source spectral density at spatial frequency* $2k\mathbf{s}_\perp$*.*

Next, we consider the case of a disk-shaped source of radius a with two (possibly different) uniform spectral densities, and with Gaussian correlation coefficients, i.e.,

$$S_i^{(0)}(\boldsymbol{\rho}) = A_i^2 \,\mathrm{circ}(\rho/\mathrm{a}), \quad (3.33)$$

where the circle function

$$\mathrm{circ}(\boldsymbol{\rho}) = \begin{cases} 1 & \text{if } |\boldsymbol{\rho}| \leq 1, \\ 0 & \text{if } |\boldsymbol{\rho}| > 1, \end{cases} \quad (3.34)$$

and

$$\mu_{ij}^{(0)}(\boldsymbol{\rho}) = B_{ij} \exp\left(-\frac{\rho^2}{2\delta_{ij}^2}\right), \quad (i, j = x, y). \quad (3.35)$$

The assumption of quasi-homogeneity implies that $a \gg \delta_{ij}$, for all i, j. The parameters A_i, B_{ij} and δ_{ij} are independent of position, but may depend on the frequency ω. They cannot be chosen arbitrarily. In particular [Wolf, 2007, Ch.9],

$$\begin{aligned} B_{xx} &= B_{yy} = 1, & (3.36)\\ B_{xy} &= B_{yx}^*, & (3.37)\\ |\mathrm{B}_{xy}| &\leq 1, & (3.38)\\ \delta_{xy} &= \delta_{yx}. & (3.39) \end{aligned}$$

To ensure that the source generates a beam-like field, the two correlation lengths δ_{xx} and δ_{yy} must satisfy the conditions (3.23) and (3.24). Finally, in order for the source to be physically realizable, its cross-spectral density matrix must be positive definite. This implies that [Gori *et al.*, 2008]

$$\sqrt{\frac{\delta_{xx}^2+\delta_{yy}^2}{2}} \leq \delta_{xy} \leq \sqrt{\frac{\delta_{xx}\delta_{yy}}{|B_{xy}|}}. \tag{3.40}$$

[Note that although Eq. (3.40) is derived in Ref. [Gori *et al.*, 2008] in the context of Gaussian Schell-model sources, it only depends on the properties of the correlation coefficients and not on those of the spectral density of the source. It therefore applies to our example.] In the present case the relevant Fourier transforms are

$$\tilde{S}_i^{(0)}(\mathbf{f}) = \frac{A_i^2 a^2}{2\pi}\frac{J_1(af)}{af}, \tag{3.41}$$

$$\tilde{S}_{xy}^{(0)}(\mathbf{f}) = \frac{A_x A_y a^2}{2\pi}\frac{J_1(af)}{af}, \tag{3.42}$$

$$\tilde{\mu}_{ij}^{(0)}(\mathbf{f}) = \frac{B_{ij}\delta_{ij}^2}{2\pi}\exp\left(-\frac{\delta_{ij}^2 f^2}{2}\right), \tag{3.43}$$

where $f=|\mathbf{f}|$ and J_1 is the Bessel function of the first kind and first order. On substituting from Eqs. (3.41)–(3.43) into Eq. (3.29), we find that

$$C_N^{(\infty)}(r\mathbf{s}_1, r\mathbf{s}_2) = 4D\left[\frac{J_1(2ka\sin\theta)}{2ka\sin\theta}\right]^2, \tag{3.44}$$

with

$$D = \frac{\sum_{i,j} A_i^2 A_j^2 |B_{ij}|^2 \delta_{ij}^4}{\left(A_x^2\delta_{xx}^2 + A_y^2\delta_{yy}^2\right)^2}, \tag{3.45}$$

and where we have made the use of the fact that $|\mathbf{s}_\perp| = \sin\theta$. From Eqs. (3.44) and (3.45) it is seen that $C_N^{(\infty)}(r\mathbf{s}_1, r\mathbf{s}_2)$ is rotationally symmetric about the z axis. We notice that the off-diagonal coefficient B_{xy} only appears in the numerator of the function D. That means that an unpolarized, quasi-homogeneous source with $|B_{xy}|=0$ has a weaker correlation of its intensity fluctuations than a partially polarized source with

$|B_{xy}| \neq 0$. This is shown in Fig. 3.3 where $C_N^{(\infty)}(r\mathbf{s}_1, r\mathbf{s}_2)$ is plotted for selected values of $|B_{xy}|$. When this parameter is nearing its upper value (blue curve), which can be calculated from Eq. (3.40), the maximum value of $C_N^{(\infty)}(r\mathbf{s}_1, r\mathbf{s}_2)$ almost reaches unity.

Another parameter that significantly influences the far-zone correlations is the ratio of the two spectral amplitudes A_x and A_y. Examples are shown in Fig. 3.4. When $A_y \gg A_x$, i.e. approaching the case of a y polarized source, the correlation reaches its maximum value of unity at $\theta = 0°$. The curve decreases with decreasing A_y until this spectral amplitude reaches about 0.7. For lower values the correlation of intensity fluctuations rises again, as the source becomes more and more like a linear polarized source, but now with its main polarization along x.

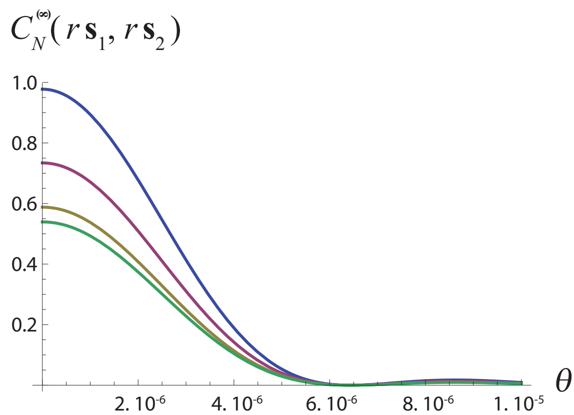

Figure 3.3: Variation of the normalized correlation of intensity fluctuations in the far-zone, as a function of the observation angle θ for different values of $|B_{xy}|$. From top to bottom: $|B_{xy}| = 0.9$ (blue), 0.6 (purple), 0.3 (olive), 0 (green). In this example $a = 3$ cm, $\delta_{xx} = 0.4$ mm, $\delta_{xy} = 0.51$ mm, $\delta_{yy} = 0.6$ mm, $A_x = 2$, $A_y = 1$, and $\lambda = 632.8$ nm.

Let us next consider a source with a rectangular shape, with sides a and b, with two uniform spectral densities, and with Gaussian correlation coefficients. In that case we have

$$S_i^{(0)}(\boldsymbol{\rho}) = A_i^2 \,\mathrm{rect}(x/a)\,\mathrm{rect}(y/b), \tag{3.46}$$

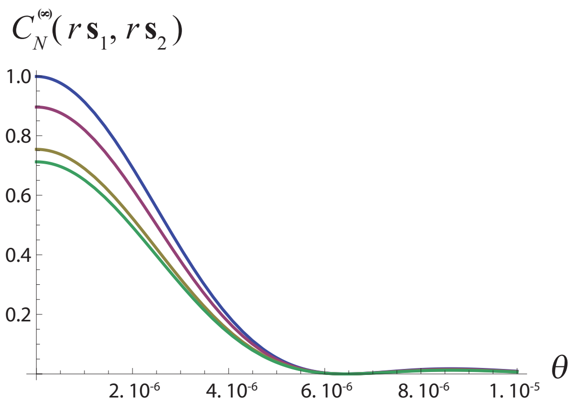

Figure 3.4: Variation of the normalized correlation of intensity fluctuations in the far-zone as a function of θ for different values of the spectral amplitude A_y, with A_x kept fixed at 1. From top to bottom: $A_y = 20$ (blue), 2 (purple), 1 (olive), 0.7 (green). In this example $A_x = 1$, $a = 3$ cm, $\delta_{xx} = 0.4$ mm, $\delta_{xy} = 0.51$ mm, $\delta_{yy} = 0.6$ mm, $|B_{xy}| = 0.6$, and $\lambda = 632.8$ nm.

with the rectangle function

$$\mathrm{rect}(x) = \begin{cases} 1 & \text{if } |x| \leq 1/2, \\ 0 & \text{if } |x| > 1/2, \end{cases} \tag{3.47}$$

and

$$\mu_{ij}^{(0)}(\boldsymbol{\rho}) = B_{ij} \exp\left(-\frac{\rho^2}{2\delta_{ij}^2}\right). \tag{3.48}$$

The assumption of quasi-homogeneity implies that $a \gg \delta_{ij}$ and $b \gg \delta_{ij}$, for all i, j. The parameters A_i, B_{ij} and δ_{ij} satisfy the same constraints as in the previous example. The pertinent Fourier transforms are now

$$\tilde{S}_i^{(0)}(\mathbf{f}) = ab\left(\frac{A_i}{2\pi}\right)^2 \operatorname{sinc}\left(\frac{f_x a}{2}\right)\operatorname{sinc}\left(\frac{f_y b}{2}\right), \tag{3.49}$$

$$\tilde{S}_{xy}^{(0)}(\mathbf{f}) = ab\frac{A_x A_y}{(2\pi)^2} \operatorname{sinc}\left(\frac{f_x a}{2}\right)\operatorname{sinc}\left(\frac{f_y b}{2}\right), \tag{3.50}$$

$$\tilde{\mu}_{ij}^{(0)}(\mathbf{f}) = \frac{B_{ij}\,\delta_{ij}^2}{2\pi}\exp\left(-\frac{\delta_{ij}^2 f^2}{2}\right), \tag{3.51}$$

where $\mathbf{f} = (f_x, f_y)$. On substituting from Eqs. (3.49)–(3.51) into Eq. (3.29), we find for the far-zone correlation of intensity fluctuations of a rectangular source the expression

$$C_N^{(\infty)}(r\mathbf{s}_1, r\mathbf{s}_2) = D\operatorname{sinc}^2(kas_x)\operatorname{sinc}^2(kbs_y), \tag{3.52}$$

with the function D defined by Eq. (3.45), and with the two directions of observation set to $\mathbf{s}_1 = (s_x, s_y, s_z)$, $\mathbf{s}_2 = (-s_x, -s_y, s_z)$. Examples of the correlation function for rectangular sources with different aspect ratios a/b are shown in Fig. 3.5. Clearly, these patterns indicate the symmetry properties of the four sources along the s_x and s_y axes.

It is interesting to compare the contours of $C_N^{(\infty)}(r\mathbf{s}_1, r\mathbf{s}_2)$ with those of the radiant intensity. From Eq. (3.16) we have that

$$J(r\mathbf{s}) = \frac{abk^2}{2\pi}(1 - s_x^2 - s_y^2)\left[A_x^2\delta_{xx}^2 e^{-\delta_{xx}^2 k^2(s_x^2+s_y^2)/2} + A_y^2\delta_{yy}^2 e^{-\delta_{yy}^2 k^2(s_x^2+s_y^2)/2}\right]. \tag{3.53}$$

The normalized radiant intensity $J(r\mathbf{s})/J(0)$ is plotted in Fig. 3.6. This far-field radiation pattern has rotational symmetry, and is independent of the aspect ratio a/b of the rectangular source: it contains no information about the shape of the source or its spectral density distribution. This is in contrast to the correlation of intensity fluctuations $C_N^{(\infty)}(r\mathbf{s}_1, r\mathbf{s}_2)$ which, as can be seen from Eq. (3.29), provides the modulus of the spatial Fourier transform of the spectral density distribution in the source plane in this particular case.

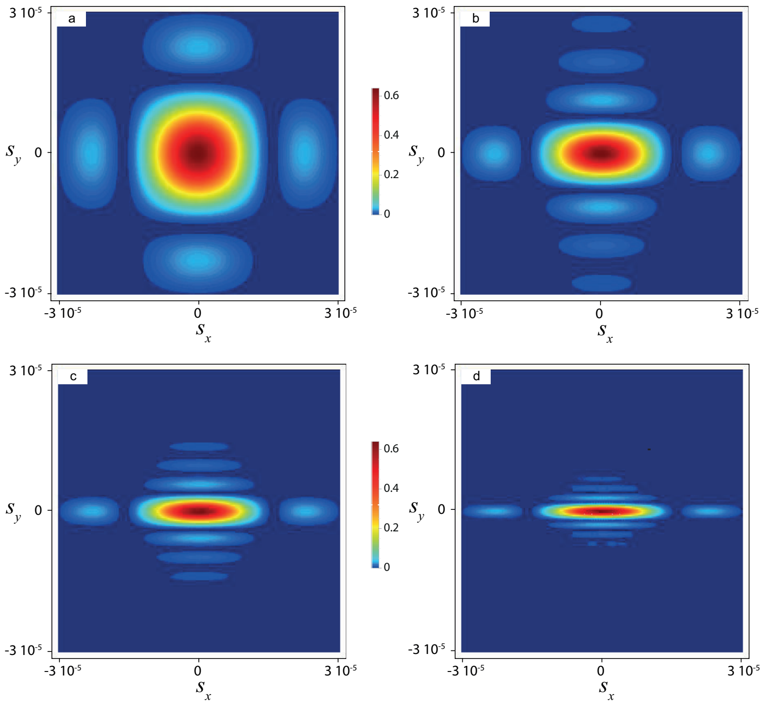

Figure 3.5: Contours of the normalized correlation of intensity fluctuations of beams generated by rectangular sources with sides a and b. The sides are chosen as $b = a$ (a), $b = 2a$ (b), $b = 4a$ (c), and $b = 8a$ (d). In these examples $A_x = 2$, $A_y = 1$, $B_{xy} = 0.2$, $\delta_{xx} = 0.4$ mm, $\delta_{yy} = 0.6$ mm, $\delta_{xy} = 0.75$ mm, $a = 2$ cm, and $\lambda = 632.8$ nm.

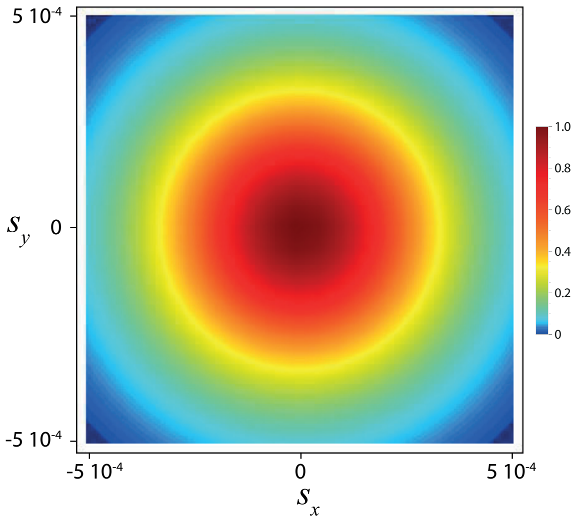

Figure 3.6: Contours of the normalized radiant intensity of beams generated by rectangular sources. The parameters are the same as in Fig. 3.5.

There is a large body of literature devoted to phase retrieval, i.e. the reconstruction of an object by knowledge of the modulus of its Fourier transform, see [Fienup, 2013] and the references therein. We demonstrate the feasibility of using the correlation of intensity fluctuations for this purpose with a simple example. Consider a partially coherent Laguerre-Gauss beam, with Gaussian correlation coefficients. Let two linear polarizers that only transmit x-polarized fields cover the intensity detectors. The relevant spectral density and the autocorrelation coefficient are then

$$S_x^{(0)}(\boldsymbol{\rho}) = A_x^2\, \rho^2 \exp(-\rho^2/2\sigma_x^2), \tag{3.54}$$

$$\mu_{xx}^{(0)}(\boldsymbol{\rho}) = \exp(-\rho^2/2\delta_{xx}^2), \tag{3.55}$$

with σ_x the effective width of the spectral density, and δ_{xx} the effective correlation length. The assumption of quasi-homogeneity implies that

$\sigma_x \gg \delta_{xx}$. Under these assumptions Eq. (3.29) reduces to the form

$$C_N^{(\infty)}(r\mathbf{s}_1, r\mathbf{s}_2) = \frac{\left|\tilde{S}_x^{(0)}(2k\mathbf{s}_\perp)\right|^2}{\left[\tilde{S}_x^{(0)}(0)\right]^2}, \quad (r_1 = r_2 = r;\, \mathbf{s}_{1\perp} = -\mathbf{s}_{2\perp} = -\mathbf{s}_\perp). \tag{3.56}$$

Since

$$\tilde{S}_x^{(0)}(\mathbf{f}) = (2 - f^2\sigma_x^2)\sigma_x^4 A_x^2 \exp(-f^2\sigma_x^2/2)/2\pi, \tag{3.57}$$

we obtain the expression

$$C_N^{(\infty)}(r\mathbf{s}_1, r\mathbf{s}_2) = (1 - 2k^2\sigma_x^2 \sin^2\theta)^2 \exp(-4k^2\sigma_x^2 \sin^2\theta). \tag{3.58}$$

The iterative method proposed in [Fienup, 1978] was used to reconstruct the spectral density distribution across the source plane from Eq. (3.58). The principal constraint for each iteration being that the object is non-negative. The contours of the spectral density $S_x^{(0)}(\boldsymbol{\rho})$ and those of the correlation of intensity fluctuations $C_N^{(\infty)}(r\mathbf{s}_1, r\mathbf{s}_2)$ are plotted in panels a and b of Fig. (3.7). From the shape of the correlation function it is seen that the source is rotationally symmetric. The initial "guess" that is used to start the iteration process is therefore taken as a random pattern with rotational symmetry, shown in panel c. The reconstructed source spectral density after 80 iterations is shown in panel d. It is seen to be very similar to the original spectral density of panel a. By rotating the two linear polarizers that cover the detectors, the distribution of $S_y^{(0)}(\boldsymbol{\rho})$ can be reconstructed in a completely similar way.

Previously proposed methods to reconstruct the source spectral density of quasi-homogeneous sources rely on far-zone measurements of the spectral degree of coherence, see [Mandel and Wolf, 1995, Sec. 5.3.3]. However, such interference experiments are quite difficult to carry out. On the other hand, measuring the correlation function $C_N^{(\infty)}(r\mathbf{s}_1, r\mathbf{s}_2)$ involves intensity measurements that are typically more robust to noise. The inversion scheme as described above may therefore offer a more practical approach for inverse imaging problems.

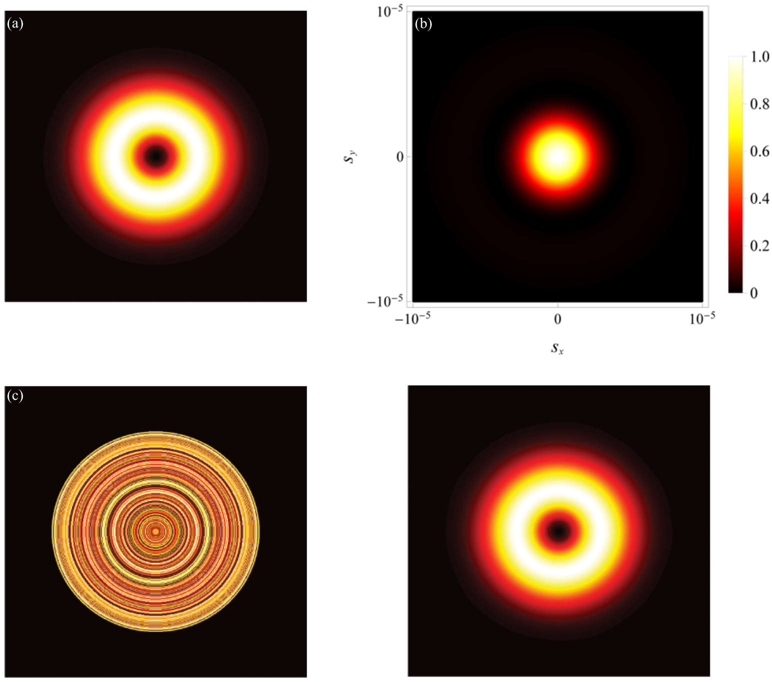

Figure 3.7: Retrieval of a simulated spectral density from its normalized correlation of intensity fluctuations in the far-zone. a: The spectral density of a partially coherent Laguerre-Gauss beam in the source plane. In this example $\lambda = 632.8$ nm and $\sigma_x = 15$ mm. b: The normalized correlation of intensity fluctuations in the far-zone. c: The initial guess for the source spectral density that is used to start the algorithm: a completely random pattern with rotational symmetry and with values between 0 and 1. d: The result of the reconstructed source spectral density after 80 iterations.

3.7 Conclusions

We have studied the correlation of intensity fluctuations in the far zone that occurs in electromagnetic beams generated by quasi-homogeneous sources. The influence of the different source parameters was investigated numerically. We found that the aspect ratio of rectangular sources with a homogeneous intensity may be determined from the correlation of intensity fluctuations. We also showed that the spectral density distribution in the source plane can be reconstructed from measurements of the Hanbury Brown-Twiss effect. This approach may find application in remote sensing and imaging.

Chapter 4

Polarization and coherence in the Hanbury Brown-Twiss effect

This Chapter is based on

- Xianlong Liu, Gaofeng Wu, Xiaoyan Pang, David Kuebel and Taco D. Visser, "Polarization and coherence in the Hanbury Brown-Twiss effect," Journal of Modern Optics, vol. 65, pp. 1437–1441 (2018).

Abstract
We study the correlation of intensity fluctuations in random electromagnetic beams, the so-called Hanbury Brown-Twiss effect (HBT). We show that not just the state of coherence of the source, but also its state of polarization has a strong influence on the far-zone correlations. Different types of sources are found to have different upper bounds for the normalized HBT coefficient.

4.1 Introduction

In their landmark experiment Hanbury Brown and Twiss studied the correlation of intensity fluctuations at two detectors with a variable separation distance, to determine the angular diameter of radio stars [Hanbury Brown and Twiss, 1954; Hanbury Brown and Twiss, 1956; Hanbury Brown, 1974]. Since then the eponymous HBT effect has been applied in many other fields, such as nuclear physics [Baym, 1998] and atomic physics [Ottl *et al.*, 2005; Schellekens *et al.*, 2005; Jeltes *et al.*, 2007]. In optics it has been used to study certain inverse problems [Kuebel *et al.*, 2013; Wu and Visser, 2014a], and to determine the mode index of vortex beams [Liu *et al.*, 2016]. It is also explored in classical versions of ghost imaging [Shirai, 2017].

In the original astronomical studies that were carried out by Hanbury Brown and Twiss, polarization issues could be ignored, and therefore a scalar description sufficed [Wolf, 2007, Ch. 7]. A generalization to random electromagnetic beams, as generated for example, by multi-mode lasers, can be found in [Mandel and Wolf, 1995, Ch. 8]. In recent years several studies were dedicated to the correlation of intensity fluctuations in such beams, among them [Shirai and Wolf, 2007] and [Al-Qasimi *et al.*, 2010], in which the degree of cross-polarization was introduced. The usefulnes of this concept has been questioned in [Hassinen *et al.*, 2011]. The evolution of the HBT effect during propagation was studied in [Li, 2014; Wu and Visser, 2014b].

In the present study we examine the far-zone HBT effect that occurs in a wide class of partially coherent beams, the so-called Electromagnetic Gaussian Schell-Model (EGSM) beams [Wolf, 2007]. As we will demonstrate, not just the state of coherence of the source, but also its state of polarization plays a major role. Also, different types of sources are found to have different upper bounds for the normalized HBT coefficient.

4.2 The HBT effect in random electromagnetic beams

We consider a stochastic, wide-sense stationary, electromagnetic beam propagating close to the z axis into the half-space $z > 0$ (see Fig. 4.1).

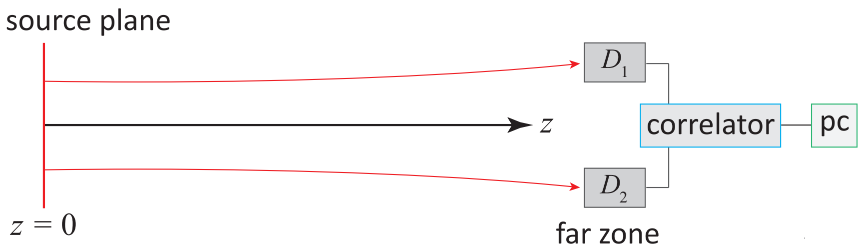

Figure 4.1: Illustrating the Hanbury Brown-Twiss experiment. D_1 and D_2 are intensity detectors, located in the far zone at $(\boldsymbol{\rho}_1, z)$ and $(\boldsymbol{\rho}_2, z)$, whose output is sent to a correlator that is connected to a pc.

$E_x(\boldsymbol{\rho}, z, \omega)$ and $E_y(\boldsymbol{\rho}, z, \omega)$ are the Cartesian components of the electric field at frequency ω along two mutually orthogonal x and y directions, perpendicular to the beam axis. The vector $\boldsymbol{\rho} = (x, y)$ denotes a transverse position. To simplify the notation, we will from here on suppress the ω dependence of the various quantities. In the space-frequency formulation of coherence theory the coherence and polarization properties of a beam at two points $\boldsymbol{\rho}_1$ and $\boldsymbol{\rho}_2$ in the same transverse plane z can be described by its cross-spectral density (CSD) matrix [Wolf, 2007]

$$\mathbf{W}(\boldsymbol{\rho}_1, \boldsymbol{\rho}_2, z) = \begin{pmatrix} W_{xx}(\boldsymbol{\rho}_1, \boldsymbol{\rho}_2, z) & W_{xy}(\boldsymbol{\rho}_1, \boldsymbol{\rho}_2, z) \\ W_{yx}(\boldsymbol{\rho}_1, \boldsymbol{\rho}_2, z) & W_{yy}(\boldsymbol{\rho}_1, \boldsymbol{\rho}_2, z) \end{pmatrix}, \tag{4.1}$$

with

$$W_{ij}(\boldsymbol{\rho}_1, \boldsymbol{\rho}_2, z) = \langle E_i^*(\boldsymbol{\rho}_1, z) E_j(\boldsymbol{\rho}_2, z)\rangle, \quad (i, j = x, y), \tag{4.2}$$

where the angled brackets denote an ensemble average. The intensity of a single realization of the beam is defined as

$$I(\boldsymbol{\rho}, z) = |E_x(\boldsymbol{\rho}, z)|^2 + |E_y(\boldsymbol{\rho}, z)|^2, \tag{4.3}$$

whereas its expectation value is given by

$$\begin{aligned} \langle I(\boldsymbol{\rho}, z)\rangle &= \langle |E_x(\boldsymbol{\rho}, z)|^2\rangle + \langle |E_y(\boldsymbol{\rho}, z)|^2\rangle && (4.4) \\ &= \mathrm{Tr}\, \mathbf{W}(\boldsymbol{\rho}, \boldsymbol{\rho}, z), && (4.5) \end{aligned}$$

where Tr denotes the trace. The intensity variation is given by the expression

$$\Delta I(\boldsymbol{\rho}, z) = I(\boldsymbol{\rho}, z) - \langle I(\boldsymbol{\rho}, z)\rangle. \tag{4.6}$$

We can introduce a measure of the correlation of intensity fluctuations at two points by defining the HBT coefficient as

$$C(\boldsymbol{\rho}_1, \boldsymbol{\rho}_2, z) = \langle \Delta I(\boldsymbol{\rho}_1, z) \Delta I(\boldsymbol{\rho}_2, z) \rangle. \tag{4.7}$$

If the source fluctuations are governed by Gaussian statistics, one can use the Gaussian moment theorem to derive that [Shirai and Wolf, 2007, Eq. (8)]

$$C(\boldsymbol{\rho}_1, \boldsymbol{\rho}_2, z) = \sum_{i,j} |W_{ij}(\boldsymbol{\rho}_1, \boldsymbol{\rho}_2, z)|^2 . \tag{4.8}$$

It is convenient to use a normalized correlation coefficient, indicated by the subscript N, namely

$$\begin{aligned} C_N(\boldsymbol{\rho}_1, \boldsymbol{\rho}_2, z) &= \frac{C(\boldsymbol{\rho}_1, \boldsymbol{\rho}_2, z)}{\langle I(\boldsymbol{\rho}_1, z) \rangle \langle I(\boldsymbol{\rho}_2, z) \rangle} \\ &= \frac{\sum_{i,j} |W_{ij}(\boldsymbol{\rho}_1, \boldsymbol{\rho}_2, z)|^2}{\operatorname{Tr} \mathbf{W}(\boldsymbol{\rho}_1, \boldsymbol{\rho}_1, z) \operatorname{Tr} \mathbf{W}(\boldsymbol{\rho}_2, \boldsymbol{\rho}_2, z)}. \end{aligned} \tag{4.9}$$

It can be shown [Hassinen *et al.*, 2011] that $0 \leq C_N(\boldsymbol{\rho}_1, \boldsymbol{\rho}_2, z) \leq 1$.

4.3 Electromagnetic Gaussian Schell-model beams

The cross-spectral density matrix elements of an EGSM beam in the source plane $z = 0$ read

$$W_{ij}(\boldsymbol{\rho}_1, \boldsymbol{\rho}_2, 0) = A_i A_j B_{ij} \exp\left[-\frac{\boldsymbol{\rho}_1^2}{4\sigma_i^2} - \frac{\boldsymbol{\rho}_2^2}{4\sigma_j^2} - \frac{(\boldsymbol{\rho}_1 - \boldsymbol{\rho}_2)^2}{2\delta_{ij}^2} \right]. \tag{4.10}$$

The source parameters A_i, B_{ij}, σ_i, and δ_{ij} are independent of position, but may depend on frequency. For their physical meaning we refer to [Gori *et al.*, 2001; Wolf, 2003b]. We will restrict ourselves to the case where the width of the spectral densities associated with E_x and E_y are equal, i.e., we assume that $\sigma_x = \sigma_y = \sigma$. The parameters have to satisfy several constraints, i.e., [WOLF, 2007, Sec. 9.4.2]

$$B_{xx} = B_{yy} = 1, \tag{4.11}$$
$$B_{xy} = B_{yx}^{*}, \tag{4.12}$$
$$|B_{xy}| \leq 1, \tag{4.13}$$
$$\delta_{xy} = \delta_{yx}. \tag{4.14}$$

Furthermore, the two conditions for the source to generate a beam-like field are [KOROTKOVA *et al.*, 2004]

$$\frac{1}{4\sigma^2} + \frac{1}{2\delta_{ii}^2} \ll \frac{2\pi^2}{\lambda^2}. \tag{4.15}$$

And finally, the non-negativeness of the cross-spectral density matrix implies that [GORI *et al.*, 2008]

$$\sqrt{\frac{\delta_{xx}^2 + \delta_{yy}^2}{2}} \leq \delta_{xy} \leq \sqrt{\frac{\delta_{xx}\delta_{yy}}{|B_{xy}|}}. \tag{4.16}$$

After propagating a distance z through free space, the CSD matrix elements evolve into (see [WOLF, 2007], where the one but last minus sign in Eq. (10) on p. 184 should be a plus sign):

$$\begin{aligned} W_{ij}(\boldsymbol{\rho}_1, \boldsymbol{\rho}_2, z) = {} & \frac{A_i A_j B_{ij}}{\Delta_{ij}^2(z)} \exp\left[-\frac{(\boldsymbol{\rho}_1 + \boldsymbol{\rho}_2)^2}{8\sigma^2 \Delta_{ij}^2(z)}\right] \\ & \times \exp\left[-\frac{(\boldsymbol{\rho}_1 - \boldsymbol{\rho}_2)^2}{2\Omega_{ij}^2 \Delta_{ij}^2(z)} + \frac{ik(\rho_2^2 - \rho_1^2)}{2R_{ij}(z)}\right], \end{aligned} \tag{4.17}$$

where

$$\frac{1}{\Omega_{ij}^2} = \frac{1}{4\sigma^2} + \frac{1}{\delta_{ij}^2}, \tag{4.18}$$

$$\Delta_{ij}^2(z) = 1 + (z/\sigma k \Omega_{ij})^2, \tag{4.19}$$

$$R_{ij}(z) = [1 + (\sigma k \Omega_{ij}/z)^2]z, \tag{4.20}$$

and $k = \omega/c$ is the wavenumber, c being the speed of light. Because we intend to study the HBT effect in the far zone of the source, we note for future use that

$$\begin{aligned} \lim_{z\to\infty} \Delta_{ij}^2(z) &= \frac{z^2}{(\sigma k \Omega_{ij})^2}, &(4.21)\\ \lim_{z\to\infty} R_{ij}(z) &= z. &(4.22)\end{aligned}$$

We will apply Eqs. (4.17), (4.21) and (4.22) to beams that are generated by different types of sources.

4.4 Unpolarized beams

For a rotationally symmetric, unpolarized source that generates an EGSM beam, we have that

$$\begin{aligned} A_x &= A_y = A, &(4.23)\\ \delta_{xx} &= \delta_{yy} = \delta, &(4.24)\\ B_{xy} &= B_{yx} = 0, &(4.25)\\ \delta_{xy} &= \delta_{yx} = 0. &(4.26)\end{aligned}$$

The two non-zero matrix elements are equal, i.e.,

$$W_{xx}(\boldsymbol{\rho}_1, \boldsymbol{\rho}_2, z) = W_{yy}(\boldsymbol{\rho}_1, \boldsymbol{\rho}_2, z) = W(\boldsymbol{\rho}_1, \boldsymbol{\rho}_2, z), \tag{4.27}$$

with, in the far zone,

$$\begin{aligned} W(\boldsymbol{\rho}_1, \boldsymbol{\rho}_2, z) = {} & \left(\frac{Ak\sigma\Omega}{z}\right)^2 \exp\left[-\frac{(\boldsymbol{\rho}_1 + \boldsymbol{\rho}_2)^2 k^2 \Omega^2}{8z^2}\right] \\ & \times \exp\left[-\frac{(\boldsymbol{\rho}_2 - \boldsymbol{\rho}_1)^2 k^2 \sigma^2}{2z^2}\right] \exp\left(\mathrm{i}k\frac{\rho_2^2 - \rho_1^2}{2z}\right), \end{aligned} \tag{4.28}$$

where

$$\frac{1}{\Omega^2} = \frac{1}{4\sigma^2} + \frac{1}{\delta^2}. \tag{4.29}$$

If we take the first reference point to be on the z axis ($\boldsymbol{\rho}_1 = \mathbf{0}$), then it is seen from Eq. (4.28) that $W(\mathbf{0}, \boldsymbol{\rho}_2, z)$ is rotationally symmetric, i.e., it depends only on $\rho_2 = |\boldsymbol{\rho}_2|$. In the far-field the polar angle $\theta \approx \tan\theta = \rho_2/z$. Hence the matrix elements can be expressed as

$$\begin{aligned} W(\mathbf{0},\theta,z) = & \left(\frac{Ak\sigma\Omega}{z}\right)^2 \exp\left(-\frac{\theta^2 k^2 \Omega^2}{8}\right) \\ & \times \exp\left(-\frac{\theta^2 k^2 \sigma^2}{2}\right) \exp\left(\mathrm{i}k\frac{\theta^2 z}{2}\right). \end{aligned} \tag{4.30}$$

Using Eq. (4.8) we obtain for the HBT coefficient the formula

$$C(\mathbf{0},\theta,z) = 2\left(\frac{Ak\sigma\Omega}{z}\right)^4 \exp\left(-\frac{\theta^2 k^2 \Omega^2}{4}\right) \exp\left(-\theta^2 k^2 \sigma^2\right). \tag{4.31}$$

From Eqs. (4.31) and (4.9) one readily finds that the normalized HBT coefficent is given by the expression

$$\begin{aligned} C_N(\mathbf{0},\theta) &= \frac{1}{2}\exp\left(\frac{\theta^2 k^2 \Omega^2}{4}\right)\exp\left(-\theta^2 k^2 \sigma^2\right) \\ &= \frac{1}{2}\exp\left(-\frac{4\theta^2 k^2 \sigma^4}{\delta^2 + 4\sigma^2}\right), \end{aligned} \tag{4.32}$$

where the z dependence has dropped out. It is evident from Eq. (4.32) that the far-zone HBT coefficient of an unpolarized, rotationally symmetric beam depends on both the effective source size σ and the correlation length δ. Also, it is seen that this coefficient has an upper bound of 1/2.

4.5 Linearly polarized beams

Let us next consider a source that is linearly polarized along the x direction. We then have

$$A_x = A, \tag{4.33}$$

$$\delta_{xx} = \delta. \tag{4.34}$$

The only non-zero matrix element, $W_{xx}(\boldsymbol{\rho}_1, \boldsymbol{\rho}_2, z)$, takes on the far-zone form

$$\begin{aligned} W_{xx}(\boldsymbol{\rho}_1,\boldsymbol{\rho}_2,z) = & \left(\frac{Ak\sigma\Omega}{z}\right)^2 \exp\left[-\frac{(\boldsymbol{\rho}_1+\boldsymbol{\rho}_2)^2 k^2 \Omega^2}{8z^2}\right] \\ & \times \exp\left[-\frac{(\boldsymbol{\rho}_2-\boldsymbol{\rho}_1)^2 k^2 \sigma^2}{2z^2}\right] \exp\left(\mathrm{i}k\frac{\rho_2^2-\rho_1^2}{2z}\right). \end{aligned} \tag{4.35}$$

As before, we take the first reference point, $\boldsymbol{\rho}_1$, to be on the z axis. Again expressing the relevant quantities in terms of the polar angle θ, we obtain for the HBT coefficient the expression

$$C(\mathbf{0},\theta,z) = \left(\frac{Ak\sigma\Omega}{z}\right)^4 \exp\left(-\frac{\theta^2k^2\Omega^2}{4}\right)\exp\left(-\theta^2k^2\sigma^2\right). \quad (4.36)$$

Hence, its normalized version

$$C_N(\mathbf{0},\theta) = \exp\left(-\frac{4\theta^2k^2\sigma^4}{\delta^2+4\sigma^2}\right). \quad (4.37)$$

It is seen that the far-zone HBT coefficient for a linearly polarized EGSM beam does not depend on the direction of polarization. Furthermore, it is twice as large as the coefficient for unpolarized light, as given by Eq. (4.32), the upper bound now being unity.

4.6 Partially polarized beams

As a third example we study a partially polarized, rotationally symmetric source. In that case

$$A_x = A_y = A, \quad (4.38)$$
$$\delta_{xx} = \delta_{yy} = \delta. \quad (4.39)$$

It immediately follows that

$$\Omega_{xx} = \Omega_{yy} = \Omega \neq \Omega_{xy}, \quad (4.40)$$
$$\Delta_{xx} = \Delta_{yy} = \Delta \neq \Delta_{xy}. \quad (4.41)$$

The two inequalities follow from the fact that, in general, $\delta_{xy} \neq \delta$. For the four matrix elements we now have the far-zone formulas

$$\begin{aligned}
W_{xx}(\boldsymbol{\rho}_1, \boldsymbol{\rho}_2, z) &= W_{yy}(\boldsymbol{\rho}_1, \boldsymbol{\rho}_2, z) \\
&= \left(\frac{Ak\sigma\Omega}{z}\right)^2 \exp\left[-\frac{(\boldsymbol{\rho}_1 + \boldsymbol{\rho}_2)^2 k^2 \Omega^2}{8z^2}\right] \\
&\times \exp\left[-\frac{(\boldsymbol{\rho}_2 - \boldsymbol{\rho}_1)^2 k^2 \sigma^2}{2z^2}\right] \exp\left(\mathrm{i}k\frac{\rho_2^2 - \rho_1^2}{2z}\right), \qquad (4.42) \\
W_{xy}(\boldsymbol{\rho}_1, \boldsymbol{\rho}_2, z) &= B_{xy} \left(\frac{Ak\sigma\Omega_{xy}}{z}\right)^2 \exp\left[-\frac{(\boldsymbol{\rho}_1 + \boldsymbol{\rho}_2)^2 k^2 \Omega_{xy}^2}{8z^2}\right] \\
&\times \exp\left[-\frac{(\boldsymbol{\rho}_2 - \boldsymbol{\rho}_1)^2 k^2 \sigma^2}{2z^2}\right] \exp\left(\mathrm{i}k\frac{\rho_2^2 - \rho_1^2}{2z}\right), \qquad (4.43) \\
W_{yx}(\boldsymbol{\rho}_1, \boldsymbol{\rho}_2, z) &= B_{xy}^* \left(\frac{Ak\sigma\Omega_{xy}}{z}\right)^2 \exp\left[-\frac{(\boldsymbol{\rho}_1 + \boldsymbol{\rho}_2)^2 k^2 \Omega_{xy}^2}{8z^2}\right] \\
&\times \exp\left[-\frac{(\boldsymbol{\rho}_2 - \boldsymbol{\rho}_1)^2 k^2 \sigma^2}{2z^2}\right] \exp\left(\mathrm{i}k\frac{\rho_2^2 - \rho_1^2}{2z}\right), \qquad (4.44)
\end{aligned}$$

where in the last expression we made use of the fact that $B_{yx} = B_{xy}^*$ and $\Omega_{yx} = \Omega_{xy}$. Taking the first reference point $\boldsymbol{\rho}_1$ on axis and expressing the relevant quantities in terms of the angle θ, we thus find for the HBT coefficient the formula

$$\begin{aligned}
C(\mathbf{0}, \theta, z) &= 2\left(\frac{Ak\sigma}{z}\right)^4 \exp\left(-\theta^2 k^2 \sigma^2\right) \qquad (4.45) \\
&\times \left[\Omega^4 \exp\left(-\frac{\theta^2 k^2 \Omega^2}{4}\right) + |B_{xy}|^2 \Omega_{xy}^4 \exp\left(-\frac{\theta^2 k^2 \Omega_{xy}^2}{4}\right)\right].
\end{aligned}$$

A straightforward calculation then yields the equations

$$\begin{aligned}
C_N(\mathbf{0},\theta) &= \frac{1}{2}\exp\left[-\theta^2k^2\left(\sigma^2-\frac{\Omega^2}{2}\right)\right] \\
&\quad\times\left\{\exp\left[-\left(\frac{\theta k\Omega}{2}\right)^2\right]+\left(\frac{\Omega_{xy}}{\Omega}\right)^4|B_{xy}|^2\exp\left[-\left(\frac{\theta k\Omega_{xy}}{2}\right)^2\right]\right\} \qquad (4.46)\\
&= \frac{1}{2}\exp\left(-\frac{4\theta^2k^2\sigma^4}{\delta^2+4\sigma^2}\right) \\
&\quad\times\left\{1+|B_{xy}|^2\left(\frac{\Omega_{xy}}{\Omega}\right)^4\exp\left[-\frac{\theta^2k^2(\Omega_{xy}^2-\Omega^2)}{4}\right]\right\}. \qquad (4.47)
\end{aligned}$$

Equation (4.47) shows that the normalized far-zone HBT coefficient of a rotationally symmetric, partially polarized source depends on its effective size σ, the two coherence lengths δ and δ_{xy}, and the parameter B_{xy}. Compared to the unpolarized case, given by Eq. (4.32), the coefficient is now larger, due to the presence of the factor between curly brackets that is always greater than unity. The upper bound now exceeds 1/2 due to the fact that $|B_{xy}| > 0$ for partially polarized sources. Clearly, a non-zero correlation between the two Cartesian components of the electric field in the source plane increases the correlation of the intensity fluctuations in the far zone. It is worth pointing out that the constraint expressed by (4.16) defines an upper limit for the value of $|B_{xy}|$.

We illustrate our results in Fig. 4.2 in which the far-zone normalized HBT coefficient is plotted for three different kinds of EGSM sources, i.e., an unpolarized source, a linearly polarized source and a partially polarized source. The coefficient for the linearly polarized case is the only with a unit upper bound, and its value always exceeds that of the other cases. The partially coherent source produces an HBT coefficent that, at all observation angles, is larger than that of its unpolarized counterpart.

4.7 Conclusions

We have examined the Hanbury Brown-Twiss effect that occurs in random beams generated by electromagnetic Gaussian Schell-model sources.

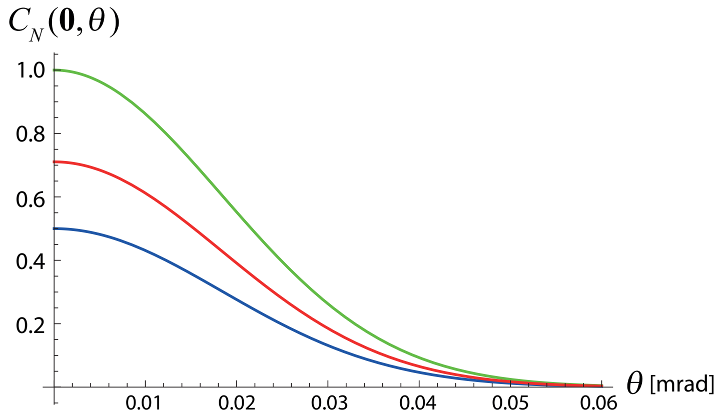

Figure 4.2: The normalized far-zone Hanbury Brown-Twiss coefficient for three EGSM sources with different states of polarization: linearly polarized (green curve), partially polarized (red curve) and unpolarized (blue curve). In these examples the parameters are: $\lambda = 632.8$ nm, $\sigma = 4$ mm, $\delta = 2$ mm, $\delta_{xy} = 2.3$ mm, and $B_{xy} = 0.5$.

Expressions for the normalized far-zone HBT coefficient were derived in terms of the source parameters. This coefficient was shown to have an upper limit that depends on the state of coherence and polarization in the source plane. Our results show that the far-zone HBT effect coefficient can be used to obtain properties of the source.

Chapter 5

A generalized Hanbury Brown-Twiss effect in partially coherent electromagnetic beams

This Chapter is based on

- Gaofeng Wu, David Kuebel and Taco D. Visser, "Generalized Hanbury Brown-Twiss effect in partially coherent electromagnetic beams," Physical Review A, vol. 99, 033846 (2019).

Abstract
The recently introduced concept of Stokes fluctuations generalizes both the Hanbury Brown-Twiss effect and the notion of scintillation. Here we apply this new framework to the specific example of a Gaussian Schell-model (GSM) beam. We derive formulas for Stokes scintillations and Stokes fluctuation correlations which explicitly express the dependence of these quantities on the GSM source parameters. It is found that the normalized Stokes scintillations vary significantly with position. Also, they can be both positively or negatively correlated.

5.1 Introduction

Recent work on intensity correlations has attempted to extend the study of the Hanbury Brown-Twiss (HBT) effect [Hanbury Brown and Twiss, 1954; Hanbury Brown and Twiss, 1956; Hanbury Brown, 1974], as customarily applied to fields of research such as astronomy and quantum optics, to the case of vector electromagnetic beams. One avenue of investigation on this topic is to explore the possible relationship between the state of polarization of the beam and the behavior of the observable HBT coefficient. Such calculations have been presented in [Shirai and Wolf, 2007; Hassinen *et al.*, 2011; Wu and Visser, 2014a; Wu and Visser, 2014b; Shirai, 2017; Liu *et al.*, 2018]. In considering the *polarization-resolved* HBT effect it seems natural to employ the traditional Stokes parameters to describe the state of polarization of the beam. However, it is trivial to observe that the HBT coefficient itself can also be expressed in terms of the first Stokes parameter, denoted by S_0. The correlation of the intensity fluctuations can therefore be thought of as a quantity that is directly related to the polarization state. Recently this observation was generalized by defining the complete class of Stokes fluctuation correlations [Kuebel and Visser, 2019]. Similarly, the scintillation coefficient, which is nothing but the local variance of S_0, can be generalized to a class of one-point correlations between the various Stokes parameters. We refer to these generalized quantities as *Stokes fluctuation correlations* and *Stokes scintillations*, respectively. Under the assumption of Gaussian statistics, a single expression for all these quantities can be derived. In this paper we apply the formalism that describes a generalized HBT experiment to a broad class of partially coherent beams, namely those of the Gaussian Schell-model type. We study how the Stokes fluctuation correlations and Stokes scintillations in the far zone are affected by the beam parameters. Both these quantities are found to display a rich behavior. For example, the normalized Stokes scintillations vary strongly with position, and their correlations can either be positive or negative.

A sketch for a generalized, polarization-resolved HBT experiment that could be used to measure the quantities of interest described in this paper is shown in Fig. 5.1. The field that is incident on the two detectors is spectrally filtered and passed through polarizing elements. The elements are chosen such that each detector measures a particular spectral Stokes

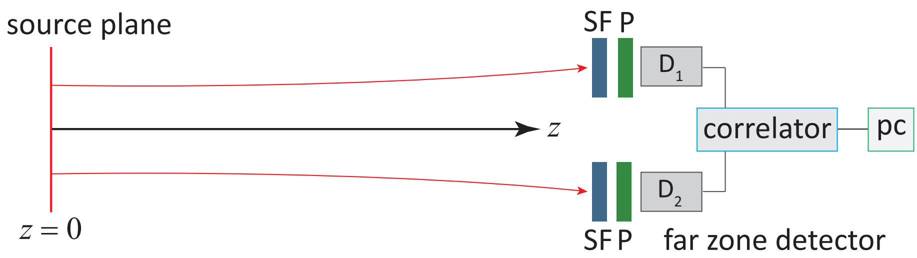

Figure 5.1: A polarization-resolved HBT experiment. The far-zone radiation of a source is passed through a narrow-band spectral filter (SF) and polarizing elements (P) that cover two intensity detectors D_1 and D_2. The output of the detectors is correlated and sent to a computer (PC).

parameter. In a traditional HBT experiment these filters and polarizers would be absent.

5.2 Stokes fluctuation correlations and Stokes scintillations

The second-order statistical properties of a partially coherent electromagnetic beam are described by its cross-spectral density matrix, which is defined as [Wolf, 2007]

$$\mathbf{W}(\mathbf{r}_1, \mathbf{r}_2, \omega) = \begin{pmatrix} W_{xx} & W_{xy} \\ W_{yx} & W_{yy} \end{pmatrix}. \tag{5.1}$$

All the matrix elements are functions of the same three variables, and given by the expression

$$W_{ij}(\mathbf{r}_1, \mathbf{r}_2, \omega) = \langle E_i^*(\mathbf{r}_1, \omega) E_j(\mathbf{r}_2, \omega) \rangle, \quad (i, j = x, y), \tag{5.2}$$

where $\mathbf{r}_1$ and $\mathbf{r}_2$ are two points of observation, ω is the angular frequency, and the angular brackets indicate an average taken over an ensemble of beam realizations.

The state of polarization of the beam is described by the four Stokes parameters [Born and Wolf, 1999]. Their average value can be expressed in terms of the cross-spectral density matrix as

$$\langle S_0(\mathbf{r},\omega)\rangle = W_{xx}(\mathbf{r},\mathbf{r},\omega) + W_{yy}(\mathbf{r},\mathbf{r},\omega), \tag{5.3}$$

$$\langle S_1(\mathbf{r},\omega)\rangle = W_{xx}(\mathbf{r},\mathbf{r},\omega) - W_{yy}(\mathbf{r},\mathbf{r},\omega), \tag{5.4}$$

$$\langle S_2(\mathbf{r},\omega)\rangle = W_{xy}(\mathbf{r},\mathbf{r},\omega) + W_{yx}(\mathbf{r},\mathbf{r},\omega), \tag{5.5}$$

$$\langle S_3(\mathbf{r},\omega)\rangle = \mathrm{i}[W_{yx}(\mathbf{r},\mathbf{r},\omega) - W_{xy}(\mathbf{r},\mathbf{r},\omega)]. \tag{5.6}$$

All preceding equations have an explicit frequency dependence, indicating that they are defined for a specific frequency component of the optical field. For brevity, we will no longer display this ω dependence from now on.

For the case of a stochastic beam the Stokes parameters are not deterministic, but they are random quantities. The fluctuations around their average value (i.e., the Stokes fluctuations) are defined as

$$\Delta S_n(\mathbf{r}) = S_n(\mathbf{r}) - \langle S_n(\mathbf{r})\rangle \quad (n = 0, 1, 2, 3), \tag{5.7}$$

where $S_n(\mathbf{r})$ is the Stokes parameter pertaining to a single realization of the beam, and $\langle S_n(\mathbf{r})\rangle$ denotes its ensemble average. We can now examine how these Stokes fluctuations are correlated. All possible pairs of their two-point correlations can be captured by introducing a 4 by 4 Stokes fluctuations correlation matrix $\mathbf{C}(\mathbf{r}_1, \mathbf{r}_2)$, whose elements are

$$C_{nm}(\mathbf{r}_1, \mathbf{r}_2) \equiv \langle \Delta S_n(\mathbf{r}_1)\Delta S_m(\mathbf{r}_2)\rangle \quad (n, m = 0, 1, 2, 3). \tag{5.8}$$

We recently showed, under the assumption that the source that generates the beam is governed by Gaussian statistics, that these elements can be expressed as [Kuebel and Visser, 2019]

$$C_{nm}(\mathbf{r}_1, \mathbf{r}_2) = \sum_{a,b}\sum_{c,d} \sigma^n_{ab}\sigma^m_{cd} W_{ad}(\mathbf{r}_1, \mathbf{r}_2) W^*_{bc}(\mathbf{r}_1, \mathbf{r}_2), \quad (a, b, c, d = x, y), \tag{5.9}$$

where $\boldsymbol{\sigma}^0$ denotes the 2 by 2 identity matrix, and the Pauli spin matrices are defined as

$$\boldsymbol{\sigma}^1 = \begin{pmatrix} 1 & 0 \\ 0 & -1 \end{pmatrix}, \quad \boldsymbol{\sigma}^2 = \begin{pmatrix} 0 & 1 \\ 1 & 0 \end{pmatrix}, \quad \boldsymbol{\sigma}^3 = \begin{pmatrix} 0 & -\mathrm{i} \\ \mathrm{i} & 0 \end{pmatrix}, \tag{5.10}$$

respectively. We remind the reader that, in contrast to the Stokes fluctuations whose correlations are described by Eq. (5.9), the Stokes parameters themselves are related by the inequality [Born and Wolf, 1999]

$$S_0^2(\mathbf{r}) \geq S_1^2(\mathbf{r}) + S_2^2(\mathbf{r}) + S_3^2(\mathbf{r}), \tag{5.11}$$

with the equal sign holding only for a fully polarized beam.

Working out Eq. (5.9) for all sixteen elements results in

$$C_{00}(\mathbf{r}_1, \mathbf{r}_2) = |W_{xx}|^2 + |W_{xy}|^2 + |W_{yx}|^2 + |W_{yy}|^2, \tag{5.12}$$

$$C_{01}(\mathbf{r}_1, \mathbf{r}_2) = |W_{xx}|^2 - |W_{xy}|^2 + |W_{yx}|^2 - |W_{yy}|^2, \tag{5.13}$$

$$C_{02}(\mathbf{r}_1, \mathbf{r}_2) = 2\,\mathrm{Re}\,[W_{xx}W_{xy}^* + W_{yy}W_{yx}^*], \tag{5.14}$$

$$C_{03}(\mathbf{r}_1, \mathbf{r}_2) = 2\,\mathrm{Im}\,[W_{yy}W_{yx}^* - W_{xx}W_{xy}^*], \tag{5.15}$$

$$C_{10}(\mathbf{r}_1, \mathbf{r}_2) = |W_{xx}|^2 + |W_{xy}|^2 - |W_{yx}|^2 - |W_{yy}|^2, \tag{5.16}$$

$$C_{11}(\mathbf{r}_1, \mathbf{r}_2) = |W_{xx}|^2 - |W_{xy}|^2 - |W_{yx}|^2 + |W_{yy}|^2, \tag{5.17}$$

$$C_{12}(\mathbf{r}_1, \mathbf{r}_2) = 2\,\mathrm{Re}\,[W_{xx}W_{xy}^* - W_{yy}W_{yx}^*], \tag{5.18}$$

$$C_{13}(\mathbf{r}_1, \mathbf{r}_2) = 2\,\mathrm{Im}\,[W_{xy}W_{xx}^* + W_{yx}W_{yy}^*], \tag{5.19}$$

$$C_{20}(\mathbf{r}_1, \mathbf{r}_2) = 2\,\mathrm{Re}\,[W_{xx}W_{yx}^* + W_{yy}W_{xy}^*], \tag{5.20}$$

$$C_{21}(\mathbf{r}_1, \mathbf{r}_2) = 2\,\mathrm{Re}\,[W_{xx}W_{yx}^* - W_{yy}W_{xy}^*], \tag{5.21}$$

$$C_{22}(\mathbf{r}_1, \mathbf{r}_2) = 2\,\mathrm{Re}\,[W_{xx}W_{yy}^* + W_{xy}W_{yx}^*], \tag{5.22}$$

$$C_{23}(\mathbf{r}_1, \mathbf{r}_2) = 2\,\mathrm{Im}\,[W_{xy}W_{yx}^* + W_{xx}^*W_{yy}], \tag{5.23}$$

$$C_{30}(\mathbf{r}_1, \mathbf{r}_2) = 2\,\mathrm{Im}\,[W_{xx}W_{yx}^* - W_{yy}W_{xy}^*], \tag{5.24}$$

$$C_{31}(\mathbf{r}_1, \mathbf{r}_2) = 2\,\mathrm{Im}\,[W_{xx}W_{yx}^* + W_{yy}W_{xy}^*], \tag{5.25}$$

$$C_{32}(\mathbf{r}_1, \mathbf{r}_2) = 2\,\mathrm{Im}\,[W_{xy}W_{yx}^* + W_{xx}W_{yy}^*], \tag{5.26}$$

$$C_{33}(\mathbf{r}_1, \mathbf{r}_2) = 2\,\mathrm{Re}\,[W_{xx}W_{yy}^* - W_{xy}W_{yx}^*], \tag{5.27}$$

where on the right-hand side the $(\mathbf{r}_1, \mathbf{r}_2)$ dependence of the cross-spectral density matrix elements W_{ij} has been suppressed for brevity. It is seen that, in the general case, all elements $C_{nm}(\mathbf{r}_1, \mathbf{r}_2)$ are non-zero. This means that the fluctuations of any Stokes parameter at a position $\mathbf{r}_1$ are correlated with the fluctuations of all four Stokes parameters at another position $\mathbf{r}_2$. As a partial check it can be verified that the expression for the first matrix element, $C_{00}(\mathbf{r}_1, \mathbf{r}_2)$, is indeed equivalent to that of the usual Hanbury Brown-Twiss coefficient [Shirai and Wolf, 2007].

When the two spatial arguments of $C_{nm}(\mathbf{r}_1, \mathbf{r}_2)$ coincide, it reduces to the Stokes scintillation matrix $D_{nm}(\mathbf{r})$, i.e.,

$$D_{nm}(\mathbf{r}) \equiv C_{nm}(\mathbf{r}, \mathbf{r}). \tag{5.28}$$

It can be derived that [Kuebel and Visser, 2019]

$$D_{00}(\mathbf{r}) = \frac{1}{2}\left[\langle S_0(\mathbf{r})\rangle^2 + \langle S_1(\mathbf{r})\rangle^2 + \langle S_2(\mathbf{r})\rangle^2 + \langle S_3(\mathbf{r})\rangle^2\right], \tag{5.29}$$

$$D_{11}(\mathbf{r}) = \frac{1}{2}\left[(\langle S_0(\mathbf{r})\rangle^2 + \langle S_1(\mathbf{r})\rangle^2 - \langle S_2(\mathbf{r})\rangle^2 - \langle S_3(\mathbf{r})\rangle^2\right], \tag{5.30}$$

$$D_{22}(\mathbf{r}) = \frac{1}{2}\left[\langle S_0(\mathbf{r})\rangle^2 - \langle S_1(\mathbf{r})\rangle^2 + \langle S_2(\mathbf{r})\rangle^2 - \langle S_3(\mathbf{r})\rangle^2\right], \tag{5.31}$$

$$D_{33}(\mathbf{r}) = \frac{1}{2}\left[\langle S_0(\mathbf{r})\rangle^2 - \langle S_1(\mathbf{r})\rangle^2 - \langle S_2(\mathbf{r})\rangle^2 + \langle S_3(\mathbf{r})\rangle^2\right]. \tag{5.32}$$

From these expressions it is seen that $D_{00}(\mathbf{r})$ is greater than or equal to the other three diagonal elements. The twelve off-diagonal elements are given by the expressions

$$D_{pq}(\mathbf{r}) = \langle S_p(\mathbf{r})\rangle\langle S_q(\mathbf{r})\rangle, \quad (p \neq q;\ \text{and } p, q = 0, 1, 2, 3). \tag{5.33}$$

It is useful to introduce a normalized version of the two correlation matrices, indicated by the superscript N, by defining

$$C^N_{nm}(\mathbf{r}_1, \mathbf{r}_2) = \frac{C_{nm}(\mathbf{r}_1, \mathbf{r}_2)}{\langle S_0(\mathbf{r}_1)\rangle\,\langle S_0(\mathbf{r}_2)\rangle}, \tag{5.34}$$

and

$$D^N_{nm}(\mathbf{r}) = \frac{D_{nm}(\mathbf{r})}{\langle S_0(\mathbf{r})\rangle^2}. \tag{5.35}$$

It can be shown that sum of the four diagonal elements of the $\mathbf{C}^N(\mathbf{r}_1, \mathbf{r}_2)$ matrix has a distinct physical meaning [Kuebel and Visser, 2019], namely

$$\sum_{m=0}^{3} C^N_{mm}(\mathbf{r}_1, \mathbf{r}_2) = 2\,|\eta(\mathbf{r}_1, \mathbf{r}_2)|^2. \tag{5.36}$$

Here $\eta(\mathbf{r}_1, \mathbf{r}_2)$ denotes the spectral degree of coherence [Wolf, 2007], the magnitude of which indicates the visibility of the interference pattern produced in Young's experiment with pinholes located at $\mathbf{r}_1$ and $\mathbf{r}_2$. Similarly, the sum of the four normalized diagonal Stokes scintillations satisfies the relation

$$\sum_{m=0}^{3} D_{mm}^{N}(\mathbf{r}) = 2. \tag{5.37}$$

The element $D_{00}^{N}(\mathbf{r})$ is equal to the square of the scintillation index [Andrews and Phillips, 2005], and is bounded, namely [Friberg and Visser, 2015]

$$\frac{1}{2} \leq D_{00}^{N}(\mathbf{r}) \leq 1. \tag{5.38}$$

It follows from Eqs. (5.33) and (5.35) that the off-diagonal elements of the $\mathbf{D}^{N}(\mathbf{r})$ matrix are also not independent. For example, $D_{23}^{N}(\mathbf{r}) = D_{02}^{N}(\mathbf{r})D_{03}^{N}(\mathbf{r})$.

In the next section we calculate the Stokes fluctuation correlations and the Stokes scintillations that occur in a specific type of beam.

5.3 Gaussian Schell-model beams

The cross-spectral density matrix elements of an electromagnetic Gaussian Schell-model (GSM) beam in its source plane, indicated by the superscript (0), are [Wolf, 2007]

$$W_{ij}^{(0)}(\boldsymbol{\rho}_1, \boldsymbol{\rho}_2) = A_i A_j B_{ij} \exp\left[-\frac{\rho_1^2}{4\sigma_i^2} - \frac{\rho_2^2}{4\sigma_j^2} - \frac{(\boldsymbol{\rho}_1 - \boldsymbol{\rho}_2)^2}{2\delta_{ij}^2}\right], \quad (i, j = x, y). \tag{5.39}$$

The parameters A_i, B_{ij}, σ_i, δ_{ij} are independent of position, but may depend on frequency. They can not be chosen freely, but have to satisfy several constraints, i.e.,

$$B_{xx} = B_{yy} = 1, \tag{5.40}$$
$$B_{xy} = B^*_{yx}, \tag{5.41}$$
$$B_{xy} = |B_{xy}|e^{\mathrm{i}\phi}, \text{with } |B_{xy}| \leq 1, \text{ and } \phi \in \mathbb{R}, \tag{5.42}$$
$$\delta_{xy} = \delta_{yx}. \tag{5.43}$$

Furthermore, the so-called realizability conditions are [Gori *et al.*, 2008]

$$\sqrt{\frac{\delta_{xx}^2 + \delta_{yy}^2}{2}} \leq \delta_{xy} \leq \sqrt{\frac{\delta_{xx}\delta_{yy}}{|B_{xy}|}}. \tag{5.44}$$

For the case $\sigma_x = \sigma_y = \sigma$, the source will generate a beam-like field if [Korotkova *et al.*, 2004]

$$\frac{1}{4\sigma^2} + \frac{1}{\delta_{xx}^2} \ll \frac{2\pi^2}{\lambda^2}, \quad \text{and} \quad \frac{1}{4\sigma^2} + \frac{1}{\delta_{yy}^2} \ll \frac{2\pi^2}{\lambda^2}. \tag{5.45}$$

On propagation to a transverse plane z the matrix elements evolve into [Wolf, 2007]

$$\begin{aligned} &W_{ij}(\boldsymbol{\rho}_1, \boldsymbol{\rho}_2, z) \\ &= \frac{A_i A_j B_{ij}}{\Delta_{ij}^2(z)} \exp\left[-\frac{(\boldsymbol{\rho}_1 + \boldsymbol{\rho}_2)^2}{8\sigma^2\Delta_{ij}^2(z)}\right] \exp\left[-\frac{(\boldsymbol{\rho}_1 - \boldsymbol{\rho}_2)^2}{2\Omega_{ij}^2\Delta_{ij}^2(z)} + \frac{ik(\rho_2^2 - \rho_1^2)}{2R_{ij}(z)}\right], \end{aligned} \tag{5.46}$$

where

$$\Delta_{ij}^2(z) = 1 + (z/\sigma k\Omega_{ij})^2, \tag{5.47}$$
$$\frac{1}{\Omega_{ij}^2} = \frac{1}{4\sigma^2} + \frac{1}{\delta_{ij}^2}, \tag{5.48}$$
$$R_{ij}(z) = [1 + (\sigma k\Omega_{ij}/z)^2]z. \tag{5.49}$$

When z tends to infinity we have

$$\Delta_{ij}^2(z) \sim \frac{z^2}{(\sigma k\Omega_{ij})^2}, \tag{5.50}$$
$$R_{ij}(z) \sim z. \tag{5.51}$$

We thus get for the far-zone elements, denoted by the superscript (∞), the expressions

$$W_{ij}^{(\infty)}(\boldsymbol{\rho}_1, \boldsymbol{\rho}_2, z) = \frac{A_i A_j B_{ij}(k\sigma\Omega_{ij})^2}{z^2} \exp\left[-\frac{(\boldsymbol{\rho}_1 + \boldsymbol{\rho}_2)^2 (k\Omega_{ij})^2}{8z^2}\right] \times \exp\left[-\frac{(\boldsymbol{\rho}_1 - \boldsymbol{\rho}_2)^2 (k\sigma)^2}{2z^2} + \frac{ik(\rho_2^2 - \rho_1^2)}{2z}\right]. \quad (5.52)$$

Let us assume, for simplicity, that the amplitude of the two spectral densities and the two autocorrelation radii are the same, i.e.,

$$A_x = A_y = A, \quad (5.53)$$

$$\delta_{xx} = \delta_{yy} = \delta. \quad (5.54)$$

This implies that

$$\Omega_{xx} = \Omega_{yy} = \Omega. \quad (5.55)$$

In the far zone the observation points are given by the polar angle $\theta \approx \tan\theta = \rho/z$. Hence we can write

$$W_{ij}^{(\infty)}(\theta, \theta, z) = K^2 B_{ij} \Omega_{ij}^2 e^{-\theta^2 k^2 \Omega_{ij}^2/2}, \quad (5.56)$$

$$W_{ij}^{(\infty)}(0, \theta, z) = K^2 B_{ij} \Omega_{ij}^2 e^{-\theta^2 k^2 \Omega_{ij}^2/8} e^{-\theta^2 k^2 \sigma^2/2} e^{ik\theta^2 z/2}, \quad (5.57)$$

where

$$K^2 = \left(\frac{Ak\sigma}{z}\right)^2. \quad (5.58)$$

We will use these two expressions to study the far-zone scintillations and the far-zone fluctuation correlations.

5.4 Stokes Scintillations

On substituting from Eq. (5.56) into Eq. (5.35), while making use of Eqs. (5.12)–(5.27), we find for the four diagonal far-zone normalized Stokes

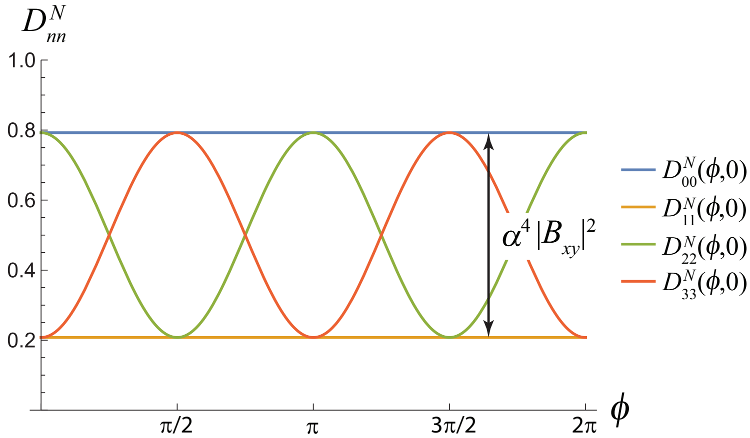

Figure 5.2: The four diagonal Stokes scintillations on the far zone axis ($\theta = 0$) as a function of the argument ϕ of the coefficient B_{xy}. In this example $\lambda = 632.8$ nm, $\sigma = 1$ cm, $\delta = 4$ mm, $\delta_{xy} = 5$ mm, and $|B_{xy}| = 0.5$.

scintillations that

$$D^N_{00}(\theta) = \frac{1}{2}\left[1 + \alpha^4 |B_{xy}|^2 e^{-\theta^2 k^2 (\Omega^2_{xy} - \Omega^2)}\right], \tag{5.59}$$

$$D^N_{11}(\theta) = \frac{1}{2}\left[1 - \alpha^4 |B_{xy}|^2 e^{-\theta^2 k^2 (\Omega^2_{xy} - \Omega^2)}\right], \tag{5.60}$$

$$D^N_{22}(\theta) = \frac{1}{2}\left[1 + \alpha^4 |B_{xy}|^2 \cos(2\phi) e^{-\theta^2 k^2 (\Omega^2_{xy} - \Omega^2)}\right], \tag{5.61}$$

$$D^N_{33}(\theta) = \frac{1}{2}\left[1 - \alpha^4 |B_{xy}|^2 \cos(2\phi) e^{-\theta^2 k^2 (\Omega^2_{xy} - \Omega^2)}\right], \tag{5.62}$$

where $\alpha \equiv \Omega_{xy}/\Omega \geq 1$. This inequality is a direct consequence of the realizability conditions Eq. (5.44). It implies that the exponential functions in Eqs. (5.59)–(5.62) all decrease with increasing θ. An example of how the on-axis Stokes scintillations may behave is presented in Fig. 5.2. There the four diagonal scintillation coefficients are plotted as a function of ϕ, the argument of the complex coeffcient B_{xy} which is defined in Eq. (5.39). Note that ϕ is the expectation value of the phase difference between E_x and E_y. The first two coefficients, D_{00} (which is the usual scintillation coefficient) and D_{11}, are independent of ϕ whereas the other two coefficients display a harmonic behavior. This can be understood as follows: the scintillations of S_0 and S_1 are, according to their definitions, only dependent on the fluctuations of $|E_x|^2$ and $|E_y|^2$ and are therefore independent of the angle ϕ. Since the other two Stokes parameters, S_2 and S_3, contain cross terms of E_x and E_y, their scintillations do depend on ϕ. Notice that although the individual Stokes scintillations may vary, their sum remains constant at two, in agreement with Eq. (5.37).

The off-diagonal scintillations can be expressed in terms of the average of the Stokes parameters, as indicated by Eq. (5.33). Using Eqs. (5.3)–(5.6) we find that

$$S_0^{(\infty)}(\theta) = 2K^2\Omega^2 \exp\left(-\frac{k^2\Omega^2\theta^2}{2}\right), \tag{5.63}$$

$$S_1^{(\infty)}(\theta) = 0, \tag{5.64}$$

$$S_2^{(\infty)}(\theta) = 2K^2\Omega_{xy}^2|B_{xy}|\cos\phi \exp\left(-\frac{k^2\Omega_{xy}^2\theta^2}{2}\right), \tag{5.65}$$

$$S_3^{(\infty)}(\theta) = 2K^2\Omega_{xy}^2|B_{xy}|\sin\phi \exp\left(-\frac{k^2\Omega_{xy}^2\theta^2}{2}\right). \tag{5.66}$$

Hence the six non-zero off-diagonal scintillation coefficients are

$$D_{02}^N(\theta) = D_{20}^N(\theta) = \alpha^2|B_{xy}|\cos\phi \exp\left[-\frac{\theta^2k^2}{2}\left(\Omega_{xy}^2 - \Omega^2\right)\right], \tag{5.67}$$

$$D_{03}^N(\theta) = D_{30}^N(\theta) = \alpha^2|B_{xy}|\sin\phi \exp\left[-\frac{\theta^2k^2}{2}\left(\Omega_{xy}^2 - \Omega^2\right)\right], \tag{5.68}$$

$$D_{23}^N(\theta) = D_{32}^N(\theta) = \alpha^4|B_{xy}|^2\cos\phi\sin\phi \exp\left[-\theta^2k^2\left(\Omega_{xy}^2 - \Omega^2\right)\right]. \tag{5.69}$$

An example is shown in Fig. 5.3. The behavior is quite distinct from that of the diagonal scintillation coefficients. Whereas for our model choice the diagonal elements are always positive, the off-diagonal scintillation coefficients can also attain negative values.

It is seen from Eqs. (5.67)–(5.69) that the off-diagonal Stokes scintillations, unlike their diagonal counterparts, do not all have the same exponential dependence on the angle of observation θ. This is illustrated in Fig. 5.4. When θ gets larger, all scintillation coefficients tend to zero, but they do so from different initial, on-axis values.

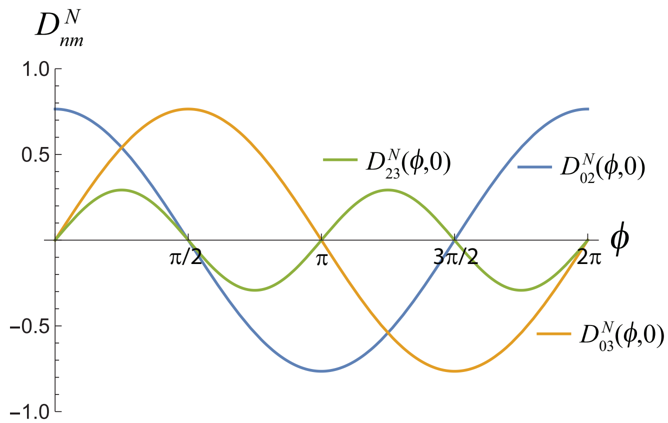

Figure 5.3: The non-zero off-diagonal Stokes scintillations on the far zone axis as a function of the argument ϕ of the coefficient B_{xy}. The parameters are the same as in Fig. 5.2.

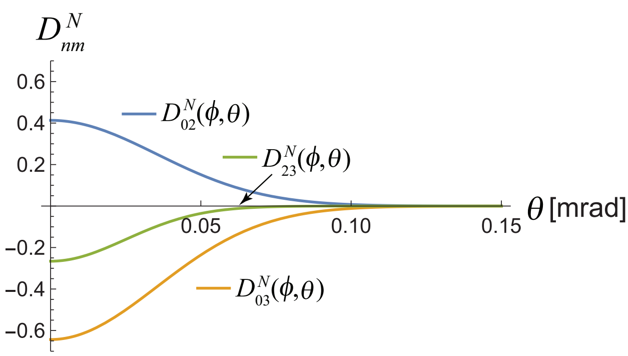

Figure 5.4: Off-diagonal Stokes scintillations in the far zone as a function of the angle of observation θ. In this example $\phi = -1.0$ rad. The other parameters are the same as in Fig. 5.2.

5.5 Stokes fluctuation correlations

For the far zone field we can use Eqs. (5.56) and (5.57) to derive the diagonal correlations of the Stokes fluctuations. The results are

$$C_{00}^N(0,\theta) = \frac{1}{2}\exp\left[-k^2\theta^2(\sigma^2 - \Omega^2/2)\right] \times \left[\exp\left(-\frac{k^2\Omega^2\theta^2}{4}\right) + \alpha^4|B_{xy}|^2 \exp\left(-\frac{k^2\Omega_{xy}^2\theta^2}{4}\right)\right], \tag{5.70}$$

$$C_{11}^N(0,\theta) = \frac{1}{2}\exp\left[-k^2\theta^2(\sigma^2 - \Omega^2/2)\right] \times \left[\exp\left(-\frac{k^2\Omega^2\theta^2}{4}\right) - \alpha^4|B_{xy}|^2 \exp\left(-\frac{k^2\Omega_{xy}^2\theta^2}{4}\right)\right], \tag{5.71}$$

$$C_{22}^N(0,\theta) = \frac{1}{2}\exp\left[-k^2\theta^2(\sigma^2 - \Omega^2/2)\right] \times \left[\exp\left(-\frac{k^2\Omega^2\theta^2}{4}\right) + \alpha^4|B_{xy}|^2 \cos(2\phi)\exp\left(-\frac{k^2\Omega_{xy}^2\theta^2}{4}\right)\right], \tag{5.72}$$

$$C_{33}^N(0,\theta) = \frac{1}{2}\exp\left[-k^2\theta^2(\sigma^2 - \Omega^2/2)\right] \times \left[\exp\left(-\frac{k^2\Omega^2\theta^2}{4}\right) - \alpha^4|B_{xy}|^2 \cos(2\phi)\exp\left(-\frac{k^2\Omega_{xy}^2\theta^2}{4}\right)\right]. \tag{5.73}$$

It is easy to show, given the constraints on the source parameters as outlined in Sec. 5.3, that these coefficients all decay exponentially as a function of the angle θ. The angular dependence of the four diagonal Stokes fluctuations coefficients is plotted in Fig. 5.5. The first coefficient, $C_{00}^N(0,\theta)$, represents the usual HBT effect (blue curve). Clearly, as can be seen from Eqs. (5.70)–(5.73), for our particular choice of a GSM beam, this coefficient is larger than the other three diagonal Stokes fluctuation correlations. As described above in Eq. (5.36), the sum of the these four coefficients is directly related to the modulus of the spectral degree of coherence $\eta(0,\theta)$. This quantity is therefore also plotted. It is seen that its angular half-width exceeds that of the four Stokes fluctuation correlations.

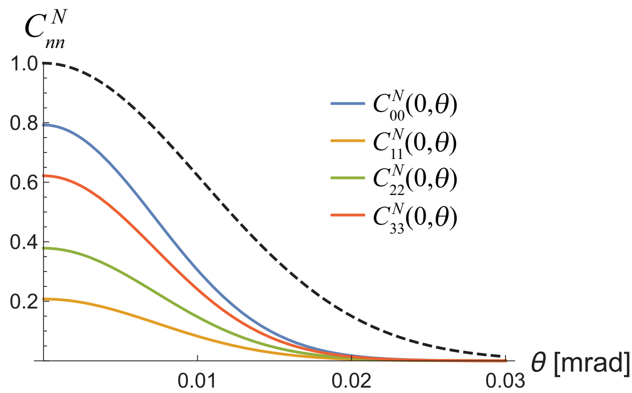

Figure 5.5: The far-zone diagonal Stokes fluctuation coefficients $C^N_{nn}(0,\theta)$ as a function of the angle θ. The argument of the coefficient B_{xy} is taken to be $\phi = -1.0$ and the other parameters are the same as in Fig. 5.2. The dashed black curve indicates the modulus of the spectral degree of coherence $\eta(0,\theta)$. The curves at $\theta = 0$ represent, in descending order, $C^N_{00}(0,\theta)$, $C^N_{33}(0,\theta)$, $C^N_{22}(0,\theta)$, and $C^N_{11}(0,\theta)$.

A direct calculation shows that only six off-diagonal elements of the $\mathbf{C}$ matrix are non-zero, with only three of them being independent, namely

$$\begin{aligned} C^N_{02}(0,\theta) &= C^N_{20}(0,\theta) \\ &= \alpha^2 \exp[-k^2\theta^2(\sigma^2 - \Omega^2/2)] \exp[-k^2\theta^2(\Omega^2 + \Omega^2_{xy})/8]|B_{xy}| \cos\phi, \end{aligned} \tag{5.74}$$

$$\begin{aligned} C^N_{03}(0,\theta) &= C^N_{30}(0,\theta) \\ &= \alpha^2 \exp[-k^2\theta^2(\sigma^2 - \Omega^2/2)] \exp[-k^2\theta^2(\Omega^2 + \Omega^2_{xy})/8]|B_{xy}| \sin\phi, \end{aligned} \tag{5.75}$$

$$\begin{aligned} C^N_{23}(0,\theta) &= C^N_{32}(0,\theta) \\ &= \frac{1}{2}\alpha^4 \exp[-k^2\theta^2(\sigma^2 - \Omega^2/2)] \exp[-k^2\theta^2\Omega^2_{xy}/4]|B_{xy}|^2 \sin(2\phi). \end{aligned} \tag{5.76}$$

Not coincidentally, the non-zero off-diagonal elements of C^N_{nm} occur for the same values of n and m as those of the D^N_{nm} matrix. They also express the same functional dependence on the modulus of B_{xy} and its angle ϕ.

5.6 Conclusions

Studies of the polarization properties of random electromagnetic beams, such as [James, 1994; Korotkova and Wolf, 2005; Korotkova *et al.*, 2005; Friberg and Visser, 2015] have typically concentrated on the degree of polarization, the Hanbury Brown–Twiss effect and scintillation. Recently the two concepts of the HBT effect and scintillation were generalized to so-called Stokes fluctuation correlations and Stokes scintillations. We examined the behavior of these sixteen new quantities in the far zone of a random beam that is generated by a Gaussian Schell-model source. It was found that the different correlations and scintillations have varying spatial distributions, and that their dependence on the source parameters differs significantly. Our results also illustrate that these quantities may non-trivially depend on the average phase difference ϕ between the two electric field components of the beam. For the specific model chosen here, for example, $D^N_{22}(\mathbf{r})$ and $D^N_{33}(\mathbf{r})$ vary sinusoidally with respect to ϕ, and the off-diagonal scintillation coefficients may be negative. Furthermore, the classical HBT coefficient is larger than the other three Stokes fluctuation correlation coefficients.

Our work shows that the HBT effect is just one of many correlations that occur in a random electromagnetic beam. These generalized HBT correlations can all be determined from intensity measurements and their values can then be used to characterize a beam in more detail than was previously done based on a single "classical" HBT measurement. They may also find application in inverse problems in which source parameters are reconstructed from far-zone observations.

Bibliography

A. Al-Qasimi, M. Lahiri, D. Kuebel, D. F. V. James, and E. Wolf, “The influence of the degree of cross-polarization on the Hanbury Brown-Twiss effect”, *Opt. Express* 18, 16, pp. 17124–17129 (2010).

L. C. Andrews and R. L. Phillips, *Laser Beam Propagation through Random Media*, Bellingham (2005).

G. Baym, “The physics of Hanbury Brown-Twiss intensity interferometry: from stars to nuclear collisions”, *Acta Phys. Pol. B* 29, pp. 1839–1884 (1998).

M. Born and E. Wolf, *Principles of Optics*, Cambridge University Press, Cambridge (1999).

W. H. Carter and E. Wolf, “Inverse problem with quasi-homogeneous sources”, *J. Opt. Soc. Am. A* 2, 11, pp. 1994–2000 (1985).

W. H. Carter and E. Wolf, “Coherence and radiometry with quasi-homogeneous planar sources”, *J. Opt. Soc. Am. A* 67, 6, pp. 785–796 (1997).

E. Collett and E. Wolf, “Beams generated by Gaussian quasi-homogeneous sources”, *Opt. Commun.* 32, 1, pp. 27–31 (1980).

J. R. Fienup, “Reconstruction of an object from the modulus of its Fourier transform”, *Opt. Lett.* 3, 1, pp. 27–29 (1978).

J. R. Fienup, “Phase retrieval algorithms: a personal tour”, *Appl. Opt.* 52, 1, pp. 45–56 (2013).

J. T. Foley and E. Wolf, “Radiometry with quasi-homogeneous sources”, *J. Mod. Opt.* 42, pp. 787–798 (1995).

A.T. Friberg and T. D. Visser, “Scintillation of electromagnetic beams generated by quasi-homogeneous sources”, *Opt. Commun.* 335, pp. 82–95 (2015).

R. J. Glauber, “The quantum theory of optical coherence”, *Phys. Rev.* 130, 6, pp. 2529–2539 (1963).

F. Gori, M. Santarsiero, R. Borghi, and V. Ramírez-Sánchez, “Realizability condition for electromagnetic Schell-model sources”, *J. Opt. Soc. Am. A* 25, 5, pp. 1016–1021 (2008).

F. Gori, M. Santarsiero, G. Piquero, R. Borghi, A. Mondello, and R. Simon, “Partially polarized Gaussian Schell-model beams”, *J. Opt. A* 3, 1, pp. 1–9 (2001).

F. Gori, M. Santarsiero, S. Vicalvi, R. Borghi, and G. Guattari, “Beam coherence-polarization matrix”, *J. Opt. A: Pure Appl. Opt.* 7, 5, pp. 941–951 (1998).

T. D. Gutierrez, “Distinguishing between Dirac and Majorana neutrinos with two-particle interferometry”, *Phys. Rev. Lett.* 96, 12, pp. 121802 (2006).

R. Hanbury Brown, *The Intensity Interferometer*, Taylor and Francis, London (1974).

R. Hanbury Brown, R. C. Jennison, and M. K. Das Gupta, “Apparent angular sizes of discrete radio sources: observations at Jodrell bank, Manchester”, *Nature* 170, pp. 1061–1063 (1952).

R. Hanbury Brown and R. Q. Twiss, “A new type of interferometer for use in radio astronomy”, *Philosophical Magazine and Journal of Science* 45, 366, pp. 663–682 (1954).

R. Hanbury Brown and R. Q. Twiss, “Correlation between photons in two coherent beams of light”, *Nature* 177, 4497, pp. 27–29 (1956).

R. Hanbury Brown and R. Q. Twiss, "Interferometry of the intensity fluctuations in light ii. an experimental test of the theory for partially coherent light", *Proceedings of the Royal Society of London. Series A, Mathematical and Physical Sciences* 234, 1234, pp. 291–319 (1958).

T. Hassinen, J. Tervo, T. Setälä, and A. T Friberg, "Hanbury Brown-Twiss effect with electromagnetic waves", *Opt. Express* 19, 16, pp. 15188–15195 (2011).

D. F. V. James, "Change of polarization of light beams on propagation in free space", *J. Opt. Soc. Am. A* 11, 5, pp. 1641–1643 (1994).

T. Jeltes, J. M. Mcnamara, W. Hogervorst, W. Vassen, V. Krachmalnicoff, M. Schellekens, and C. I. Westbrook, "Comparison of the Hanbury Brown-Twiss effect for bosons and fermions", *Nature* 445, 7216, pp. 402 (2007).

K. Kim and E. Wolf, "Propagation law for Walther's first generalized radiance function and its short-wavelength limit with quasi-homogeneous sources", *J. Opt. Soc. Am. A* 4, 7, pp. 1233–1236. (1987).

O. Korotkova, M. Salem, and E. Wolf, "Beam conditions for radiation generated by an electromagnetic Gaussian Schell-model source", *Opt. Lett.* 29, 11, pp. 1173–1175 (2004).

O. Korotkova, T. D. Visser, and E. Wolf, "Polarization properties of stochastic electromagnetic beams", *Opt. Commun.* 281, pp. 35–43 (2005).

O. Korotkova and E. Wolf, "Changes in the state of polarization of a random electromagnetic beam on propagation", *Opt. Commun.* 246, 1-3, pp. 35–43 (2005).

D. Kuebel and T. D. Visser, "Generalized Hanbury Brown-Twiss effect for Stokes parameters", *J. Opt. Soc. Am. A* 36, 3, pp. 362–367 (2019).

D. Kuebel, T. D. Visser, and E. Wolf, "Application of the Hanbury Brown-Twiss effect to scattering from quasi-homogeneous media", *Opt. Commun.* 294, pp. 43–48 (2013).

Y. Li, “Correlations between intensity fluctuations in stochastic electromagnetic Gaussian Schell-model beams”, *Opt. Commun.* 316, pp. 67–73 (2014).

Y. Li and E. Wolf, “Radiation from anisotropic Gaussian Schell-model sources”, *Opt. Lett.* 7, 6, pp. 256–258 (1982).

R. Liu, F. Wang, D. Chen, Y. Wang, Y. Zhou, H. Gao, P. Zhang, and H. Li, “Measuring mode indices of a partially coherent vortex beam with Hanbury Brown and Twiss type experiment”, *Appl. Phys. Lett.* 108, 5, pp. 051107 (2016).

X. Liu, G. F. Wu, X. Pang, D. Kuebel, and T. D. Visser, “Polarization and coherence in the Hanbury Brown-Twiss effect”, *J. Mod. Opt.* 65, 12, pp. 1437–1441 (2018).

L. Mandel and E. Wolf, *Optical Coherence and Quantum Optics*, Cambridge University Press, Cambridge (1995).

A. Michelson and F. G. Pease, “Measurement of the diameter of α orionis with the interferometer”, *The Astrophysical Journal* 53, pp. 249–259 (1921).

A. Öttl, S. Ritter, M. Köhl, and T. Esslinger, “Correlations and counting statistics of an atom laser”, *Phys. Rev. Lett.* 95, 9, pp. 090404 (2005).

S. B. Raghunathan, H. F. Schouten, and T. D. Visser, “Correlation singularities in partially coherent electromagnetic beams”, *Opt. Lett.* 37, 20, pp. 4179–4181 (2012).

S. B. Raghunathan, T. D. Visser, and E. Wolf, “Far-zone properties of electromagnetic beams generated by quasi-homogeneous sources”, *Opt. Commun.* 295, pp. 11–16 (2013).

H. Roychowdhury and E. Wolf, “Determination of the electric cross-spectral density matrix of a random electromagnetic beam”, *Opt. Commun.* 226, 1-6, pp. 57–60 (2003).

M. Schellekens, R. Hoppeler, A. Perrin, J. V. Gomes, D. Boiron, A. Aspect, and C. I. Westbrook, "Hanbury Brown-Twiss effect for ultracold quantum gases", *Science* 310, 5748, pp. 648–651 (2005).

T. Shirai, "Modern aspects of intensity interferometry with classical light", *Progress in Optics* 62, pp. 1–72 (2017).

T. Shirai and E. Wolf, "Coherence and polarization of electromagnetic beams modulated by random phase screens and their changes on propagation in free space", *J. Opt. Soc. Am. A* 21, 10, pp. 1907–1916 (2004).

T. Shirai and E. Wolf, "Correlations between intensity fluctuations in stochastic electromagnetic beams of any state of coherence and polarization", *Opt. Commun.* 272, 2, pp. 289–292 (2007).

T. D. Visser, D. G. Fischer, and E. Wolf, "Scattering of light from quasi-homogeneous sources by quasi-homogeneous media", *J. Opt. Soc. Am. A* 23, 7, pp. 1631–1638 (2006).

T. D. Visser, D. Kuebel, M. Lahiri, T. Shirai, and E. Wolf, "Unpolarized light beams with different coherence properties", *J. Mod. Opt.* 56, 12, pp. 1369–1374 (2009).

S. N. Volkov, D. F. V. James, T. Shirai, and E. Wolf, "Intensity fluctuations and the degree of cross-polarization in stochastic electromagnetic beams", *J. Opt. A Pure Appl. Opt.* 10, 5, pp. 055001 (2008).

E. Wolf, "Correlation-induced changes in the degree of polarization, the degree of coherence, and the spectrum of random electromagnetic beams on propagation", *Opt. Lett.* 28, 13, pp. 1078–1080 (2003a).

E. Wolf, "Unified theory of coherence and polarization of random electromagnetic beams", *Phys. Lett. A* 312, 5-6, pp. 263–267 (2003b).

E. Wolf, *Introduction to the Theory of Coherence and Polarization of Light*, Cambridge University Press, Cambridge (2007).

E. Wolf and W. H. Carter, “Fields generated by homogeneous and by quasi-homogeneous planar secondary sources”, *Opt. Commun.* 50, 3, pp. 131–136 (1984).

G. Wu and T. D. Visser, “Correlation of intensity fluctuations in beams generated by quasi-homogeneous sources”, *J. Opt. Soc. Am. A* 31, 10, pp. 2152–2159 (2014a).

G. Wu and T. D. Visser, “Hanbury Brown-Twiss effect with partially coherent electromagnetic beams”, *Opt. Lett.* 39, 9, pp. 2561–2564 (2014b).

Summary in Dutch

De Nederlandse titel van dit proefschrift luidt: Het Hanbury Brown-Twiss effect in elektromagnetische bundels. Dit effect treedt op in velden die niet determistisch zijn, zoals de straling van sterren of van multi-mode lasers. Het beschrijft de correlatie tussen de intensiteitsfluctuaties die gemeten worden door twee detectoren. Naarmate de afstand tussen de detectoren groter wordt, zal deze correlatie geleidelijk minder sterk worden. De oorspronkelijke toepassing, in de jaren vijftig van de twintigste eeuw, betrof de bestudering van radiosterren. Als zo een ster vele lichtjaren ver weg staat, is het niet mogelijk om door middel van een directe meting de grootte ervan te bepalen. Met behulp van de HBT techniek kan dat echter wel. Door de afname van de correlatie te plotten als functie van de afstand tussen de beide detectoren kan, door gebruik te maken van het van Cittert-Zernike theorema, de straal van de ster vastgesteld worden. De afgelopen zeventig jaar zijn allerlei varianten van de HBT correlaties succesvol toegepast in andere takken van de natuurkunde, zoals kernfysica, atoomfysica en kwantum optica.

Dit proefschrift is gebaseerd op vier studies van het Hanbury Brown-Twiss effect in stochastische, elektromagnetische bundels. In Hoofdstuk 1 wordt de benodigde wiskundige achtergrond, de zogenaamde coherentie theorie, beschreven.

Hoofdstuk 2 behandelt hoe een stochastische bron straling uitzendt waarin verschillende correlaties geleidelijk aan worden opgebouwd als het veld zich voortplant. Het blijkt dat de tweede-orde correlaties een eenvoudiger gedrag vertonen dan vierde-orde correlaties zoals het HBT effect.

In hoofdstuk 3 wordt een speciaal type bron beschreven, de zogeheten quasi-homogene bron. Dat is, simpel gezegd, een bron waarvan de ruimtelijke coherentielengte veel kleiner is dan de afmetingen van de bron zelf. Voor zulke bronnen zijn recentelijk reciprociteitsrelaties afgeleid. Deze relaties beschrijven de statistische eigenschappen van het verre veld in termen van de bronparameters. Ze kunnen ook worden gebruikt om het HBT effect te analyseren. Dit leidt tot een nieuwe aanpak van een inverse probleem: de bepaling van de vorm van een bron door middel van het HBT effect in het verre veld.

Het HBT effect voor het veld van een brede klasse van stochastische bronnen, de zogenaamde Gauss-Schell bronnen, staat centraal in Hoofdstuk 4. De invloed van de polarisatietoestand van de bron op de maximale sterkte van de correlatie wordt in kaart gebracht door middel van analytische en numerieke technieken.

Het laatste Hoofdstuk, nummer 5, laat zien dat het HBT effect eigenlijk één bijzondere vorm is van een bredere klasse van zogenaamde Stokes fluctuatie correlaties. Ook de klassieke notie van een scintillatie coëfficient kan worden veralgemeniseerd tot een Stokes scintillatie. Het blijkt dat deze gegeneraliseerde correlaties en scintillaties niet onafhankelijk zijn, maar verbonden zijn door somregels. Deze resultaten worden geïllustreerd voor een brede klasse van stochastische, elektromagnetische bundels.

Acknowledgments

First and foremost, I would like to express my sincere gratitude to my excellent advisor: Prof. Dr. Taco D. Visser for his supervision. As a theoretical physicist, he is always professional, curious, creative, critical and has a broad knowledge. Thank you for training my physical thinking and guiding me to thoroughly understanding the coherence theory. Furthermore, I also would like to thank you for riding in suburbs and walking in the seaside with me. It makes me very happy to enjoy the beautiful scenery of Amsterdam. I would like to thank Prof. Dr. Yangjian Cai for giving me the opportunity and introducing me to study with Taco. I would also like to thank Prof. Dr. B. J. Hoenders for introducing me to study with Taco and for warmly inviting me to visit the Groningen.

Second, I would like to thank my thesis reading committee for their valuable comments. I would also like to thank the China Scholarship Council (CSC) for supporting me to pursue my Ph.D.

Third, I would like to thank my nice room mates Xinnan Lin and Hecheng Zhang for the enjoyable time we had at Lelylaan. I will remember those happiness forever that we lived in the same house together.

I would like to thank my friends Guangquan, Zhiqing, Yongjie, Wenjin, Ting for their help in Amsterdam and the great time that we had in Amsterdam. I wish you success with your work in the future.

Lastly, I would like to thank my parents for the years of unconditional love and support. I would also like to thank my wife for her love and giving too much to the whole family. In particular, I would like to thank my wife for bringing a new life, my lovely son, to my family.

Gaofeng Wu
March 2019